TABLE 1 Description of acute controllers ($n = 10$)[a]

Participant	HLAs	eDPI[b] (pVL[c])	
		Initial	Follow-up
AC01	A*01:01/A*31:01; B*37:01/B*51:09; C*01:02/C*06:02	33 (25,000)	383 (50)
AC02	A*02:01/A*32:01; B*35/B*44; C*04:01/C*05	72 (15,200)	469 (774)
AC03	A*02:01/A*24:01; B*15:01/B*41:01; C*03/C*17	86 (1,490)	
AC04	A*02:01/A*24:02; B*27:05/B*35:12; C*01:02/C*01:02	72 (1,140)	251 (50)
AC05	A*24:02/A*31:01; B*39:01/B*52:01; C*07:02/C*12:02	71 (7,160)	587 (250)
AC06	A*01:01/A*02:01; B*44:02/B*57:01; C*05/C*06:02	135 (440)	
AC07	A*25:01/A*68:01; B*18:01/B*57:01; C*06:02/C*12:03	98 (23,900)	204 (1,720)
AC08	A*02:01/A*31:01; B*08:01/B*44:02; C*05/C*07	102 (572)	
AC09	A*01:01/A*68:02; B*08:01/B*44:02; C*05/C*07	52 (45,700)	268 (110)
AC10	A*01:01/A*01:01; B*15:17/B*49:01; C*07:01/C*12:03	59 (22,200)	

[a] Abbreviations: HLA, human leukocyte antigen; eDPI, estimated number of days postinfection; pVL, plasma viral load at baseline.
[b] Median (IQR) eDPI for AC ($n = 10$) at baseline, 72 (57 to 99). Median (IQR) eDPI for all AP ($n = 50$) at baseline, 56 (39 to 75) ($P = 0.07$). Median (IQR) eDPI for AP > 40 eDPI ($n = 37$) at baseline, 72 (53 to 88) ($P = 0.4$). *P* values represent Mann-Whitney comparisons to AC cohort.
[c] Median (IQR) pVL in numbers of HIV RNA copies per milliliter for AC ($n = 10$) at baseline, 11,180 (998 to 24,175). Median (IQR) pVL for all AP ($n = 50$) at baseline, 337,500 (35,925 to 750,100) ($P < 0.001$). Median (IQR) pVL for AP > 40 eDPI ($n = 37$) at baseline, 186,000 (22,350 to 750,005) ($P < 0.001$). *P* values represent Mann-Whitney comparisons to AC cohort.

described previously (52), with modifications as follows. Total cell lysates were subjected to SDS-PAGE using Mini-Protean TGX 4% to 20% gels (Bio-Rad Laboratories), and proteins were electroblotted onto a polyvinylidene difluoride (PVDF) membrane. Nef protein was detected using a polyclonal rabbit (catalog no. 2949; NIH AIDS Reagent Program) (1:4,000) (54) or sheep (catalog. no. ARP444; NIBSC Center for AIDS Reagents) (1:2,000) antibody followed by staining with secondary donkey anti-rabbit (GE Healthcare) (1:30,000) or anti-sheep (Jackson ImmunoResearch) (1:35,000) antibody. For all experiments, expression of beta-actin was assessed simultaneously using primary mouse anti-actin (Sigma) (1:20,000) and secondary goat anti-mouse (Jackson ImmunoResearch) (1:20,000) antibodies. Band intensities were quantified with ImageQuant LAS 400 (GE Healthcare) and compared to the positive-control SF2 Nef values.

Site-directed mutagenesis. *nef* variants were generated using a QuikChange II site-directed mutagenesis kit (Stratagene) according to the manufacturer's instructions or using a PCR-based overlap extension method (55). Mutations were validated by bidirectional sequencing of the full-length *nef* insert prior to functional analysis.

Statistics. Statistical analyses were conducted in Prism 5.0 (Graphpad Software, Inc.). The Mann-Whitney U test was used to compare Nef functions between groups. In patients with longitudinal (baseline versus follow-up) Nef functional assessments, the Wilcoxon paired test was employed. Spearman's correlation was used to investigate relationships between different Nef functions or samples with clinical HIV-1 parameters (e.g., CD4 T-cell count and plasma viral load). All tests were two-tailed, with $P < 0.05$ considered statistically significant.

Nucleotide sequence accession numbers. All unique clonal *nef* sequences from AC have been deposited in GenBank (accession numbers KJ996014 to KJ996066).

RESULTS

Isolation of early Nef clones from HIV-1 controllers and progressors. Clinical data from HIV-1-infected individuals enrolled at sites in the United States, Germany, and Australia were retrospectively screened to identify persons with acute/early infection who subsequently maintained viremia control below 2,000 RNA copies/ml during the first year postinfection and for whom a baseline sample within 150 days of their estimated date of infection was available for study (32) (Fig. 1). A comparison group of 50 acute progressors (AP) enrolled at the same sites who displayed pVL of greater than 2,000 RNA copies/ml over a similar period of time were also assessed. Consistent with a previous study undertaken in this cohort (32), no significant enrichment of protective HLA class I alleles was observed in AC compared to AP (e.g., HLA-B*57 prevalence was 20% in AC versus 10% in AP; Fisher's exact test $P = 0.3$) (data not shown).

The times of baseline sample collection differed slightly between cohorts: for AC, samples were collected a median of 72 (interquartile range [IQR], 57 to 99) days following the estimated infection date, while those for AP were collected a median of 56 (IQR, 39 to 75) days postinfection (Mann-Whitney test; $P = 0.065$) (Table 1). Baseline pVL was also significantly lower in AC, which is not surprising given that these patients were selected based on their ability to subsequently control viremia. Nevertheless, we were concerned that differences in baseline pVL could have been due in part to the earlier enrollment times for AP (who thus had a higher likelihood of being sampled closer to the time of peak viremia) and that this could potentially bias downstream analyses. Exclusion of AP with the earliest enrollment times (prior to 40 days postinfection) allowed us to identify a subset of 37 AP with baseline sample dates (median, 72 [IQR, 53 to 88] days) that were comparable to those of AC ($P = 0.42$) (Table 1). For the remainder of our study, all primary analyses were performed on the entire AP cohort, with secondary analyses performed using the AP subset matched for the enrollment date. Results were consistent in all cases, even when not explicitly indicated in the text.

Participant-derived *nef* alleles were amplified from baseline plasma by nested RT-PCR and sequenced. As expected from an acutely infected population, the median number of amino acid mixtures observed in bulk Nef HIV sequences was low: a median of 0 (IQR, 0 to 1) for AC compared to 0 (IQR, 0 to 2) for AP ($P = 0.3$). Nef amplicons were cloned into a cytomegalovirus (CMV) expression plasmid, and individual clones were isolated and resequenced to confirm an intact Nef open reading frame. For each AC, a minimum of 5 baseline *nef* clones (median, 7; range, 5 to 13) were isolated and sequenced. For each AP, 1 to 13 baseline clones (median, 2) were isolated and sequenced. All clones were HIV-1 subtype B. Each Nef clone was verified to cluster closely with the original bulk plasma HIV RNA sequence (see Fig. S1 in the supplemental material). Overall, the median number of amino acid differences between the clonal and original bulk sequences was 0 (IQR, 0 to 1) for both AC and AP. For each patient, the first

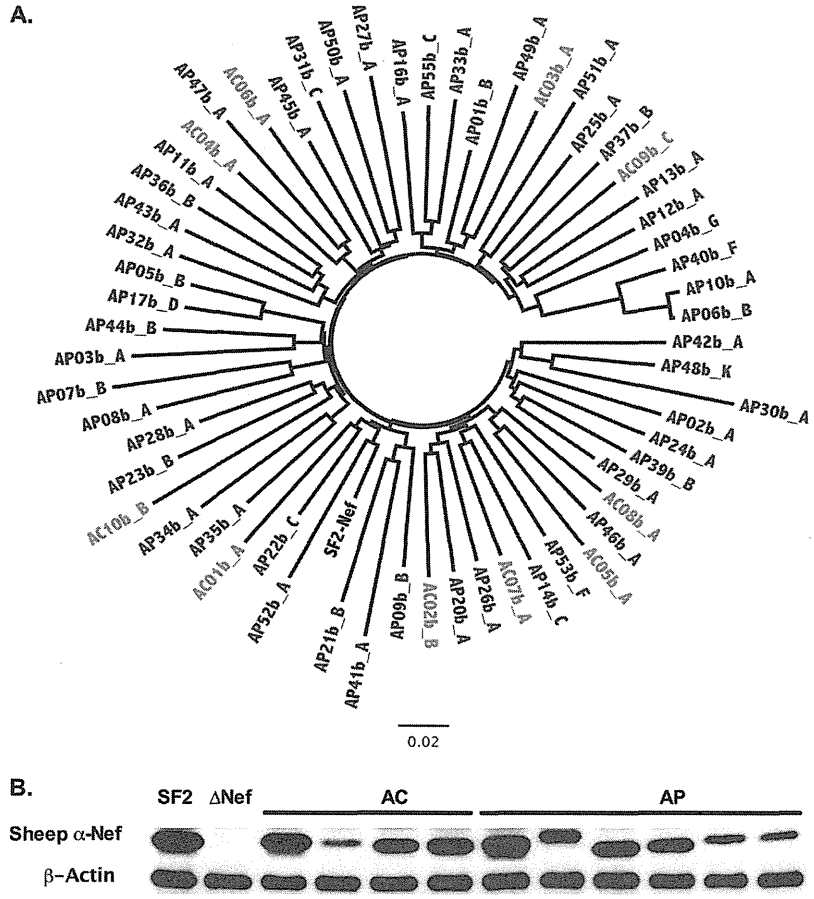

FIG 2 Nef sequences from AC and AP display no substantial phylogenetic clustering. (A) An unrooted maximum-likelihood phylogenetic tree depicts the representative Nef clone isolated from 10 AC (red) and 50 AP (blue), indicating that sequences did not exhibit substantial clustering by cohort. The HIV-1_{SF2} Nef sequence (black) is included for comparison. A phylogenetic tree that includes all clonal Nef sequences used for this study is shown in Fig. S1 in the supplemental material. (B) Western blot analysis was used to examine steady-state protein levels in AC and AP Nef clones, along with Nef_{SF2} (positive control) and ΔNef (negative control). β-Actin was used as a cellular protein control.

isolated clone was arbitrarily designated a "representative clone," while the most frequently observed clone was designated the "predominant clone" (see Fig. S1). AC and AP *nef* sequences did not display substantial intracohort clustering in a combined phylogeny (Fig. 2A; see also Fig. S1), consistent with previous analyses of *gag* and *pol* genes from these persons (32). Together with previous results, our data indicate that early HIV-1 control in AC is unlikely to be due to gross HIV sequence defects or recent descent from a common attenuated viral ancestor. We confirmed Nef expression by Western blotting for the predominant clone isolated from all 10 AC and compared detection levels to those of a random subset of 10 AP. No significant differences in band intensity were observed between cohorts (representative data shown in Fig. 2B), suggesting that Nef proteins from AC exhibited *in vitro* stability comparable to the stability of those from AP.

Nef clones from AC display impaired CD4 and HLA class I downregulation function. The ability of Nef clones to downregulate cell surface CD4 and HLA class I molecules was examined at 24 h following transfection using flow cytometry (Fig. 3). For each AC, the function of 2 to 5 unique clones was assessed. Results were normalized to those of a positive control ($SF2_{Nef}$) that displays strong CD4 and HLA class I downregulation activities (21, 56) such that values less than 1.0 indicate lower Nef function and values greater than 1.0 indicate higher Nef function relative to $SF2_{Nef}$. A negative-control plasmid lacking *nef* did not downregulate either surface protein (Fig. 3A and B); as such, its activity is 0 in this assay. Based on an assessment of a representative clone isolated from each individual, the ability of Nef to downregulate CD4 in AC (median, 0.94 [IQR, 0.87 to 0.98]) was modestly lower than that observed in AP (0.99 [0.97 to 1.02]) ($P = 0.004$) (Fig. 3C). In addition, HLA class I downregulation activity was markedly lower in AC (0.83 [0.65 to 0.93]) than in AP (1.00 [0.94 to 1.06]) ($P < 0.001$) (Fig. 3D). Secondary analyses using the "date-of-enrollment-matched" AP subset were consistent with a lower function of AC compared to that seen with AP Nefs (CD4, $P = 0.01$; HLA, $P = 0.001$; data not shown), indicating that our findings are not attributable simply to biases related to the sample collection date. Similarly, analyses comparing the median downregulation functions of all Nef clones isolated in AC versus AP also indicated significantly lower activities in the latter group (CD4, $P = 0.01$; HLA, $P < 0.001$; Fig. S2 in the supplemental material and data not shown), suggesting that our observations were not

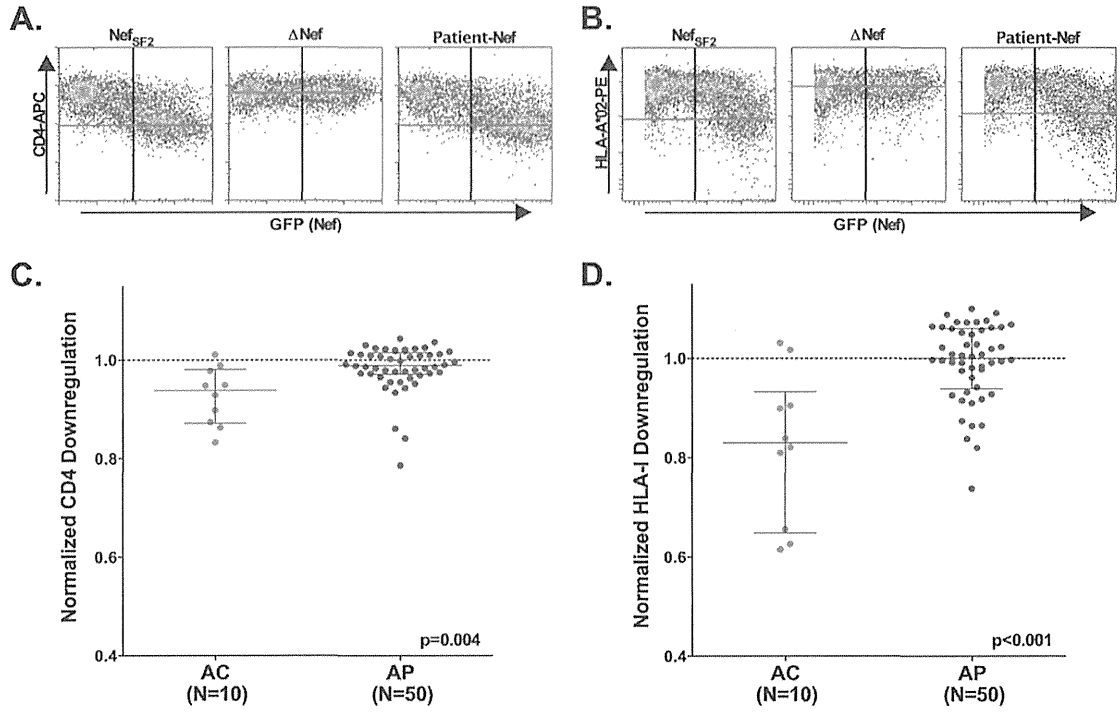

FIG 3 Reduced *in vitro* function is observed for AC Nef clones. Nef CD4 and HLA class I downregulation functions were assessed in ≥3 replicates, using flow cytometry. (A and B) Representative flow cytometry plots display relative levels of downregulation of CD4 (A) and HLA class I (B) for CEM-A*02^{+} cells transfected with Nef$_{SF2}$ (positive control) or ΔNef (negative control) or for one participant-derived Nef clone. The *x* axis (GFP^{+}) indicates transfected cells, and the *y* axis indicates surface expression of CD4 or HLA class I molecules. (C and D) Scatter plots depict normalized CD4 (C) or HLA class I (D) downregulation activities in representative Nef clones from AC (n = 10, red) compared to downregulation activities in those from AP (n = 50, blue). A dashed line (---) in each panel illustrates normalized activity of 1.0, which represents the function of Nef$_{SF2}$. Values below 1.0 indicate lower function relative to Nef$_{SF2}$, while values above 1.0 indicate higher Nef function.

driven by biases related to analyses of only a single clone per patient. Together, these results suggest that Nef-mediated HLA downregulation (and, to a lesser extent, CD4 downregulation) may contribute to early viremia control.

Nef clones from AC show reduced ability to enhance virion infectivity. We next constructed recombinant NL4.3 viruses encoding a representative early clonal *nef* sequence from 10 AC and 41 AP and assessed virion infectivity. No difference in viral production between stocks containing AC and AP *nef* sequences was observed, as determined by p24^{Gag} ELISA, although there was a trend toward higher values among AC-derived viruses (Fig. 4A). TZM-bl cells were inoculated with virus (3 ng p24^{Gag}), and infectivity was measured at 48 h postinfection using chemiluminescence assays. Data were normalized to a positive-control virus, NL4.3-*nef*$_{SF2}$, as described above. All recombinant viral stocks displayed infectivity values greater than those determined for the NL4.3Δ*nef* negative control, whose mean activity was 0.02 (standard deviation, 0.009; n = 8 replicates) in this assay. Overall, viruses encoding AC-derived *nef* alleles displayed significantly lower infectivity values (median, 0.59 [IQR, 0.44 to 0.71]) compared to those from AP (1.16 [0.71 to 1.51]) (P = 0.003) (Fig. 4B). Results were consistent in a secondary analysis using "date-of-enrollment-matched" AP clones (P = 0.01; data not shown).

HLA class I downregulation activity correlates with baseline clinical parameters in AC. We next wanted to characterize the relationship between these three Nef functions and markers of clinical status in the AC and AP cohorts (Table 2 and Table 3, respectively; see also Fig. S3 in the supplemental material). As expected for samples obtained during early infection following peak viremia, pVL correlated inversely with the estimated number of days postinfection in both AC (Spearman R = −0.77, P = 0.01) and AP (R = −0.38, P = 0.007). Consistent with previous observations in other cohorts (21, 56, 57), Nef CD4 and HLA class I downregulation functions correlated positively in both AC (R = 0.74, P = 0.02) and AP (R = 0.56, P < 0.001). Given that these activities are largely genetically separable in mutational studies of HIV-1 reference strains (58, 59), this result supports the idea of the existence of secondary genetic determinants lying outside critical motifs in patient-derived Nef isolates that may modulate function and/or protein stability. Of note, the ability of Nef to enhance virion infectivity correlated significantly with baseline pVL in AP (R = 0.54, P < 0.001) but not AC. This may have been due to the generally low activity seen among AC clones for this function, but it warrants further investigation. Surprisingly, Nef's HLA class I downregulation activity correlated inversely with estimated numbers of days postinfection (R = −0.85, P = 0.004) and positively with pVL (R = 0.81, P = 0.007) in AC. Similar associations were not seen for AP, despite enhanced statistical power to observe differences in this group. Together, these results suggest that longitudinal alterations in Nef function may contribute to spontaneous HIV-1 control in AC but not in AP.

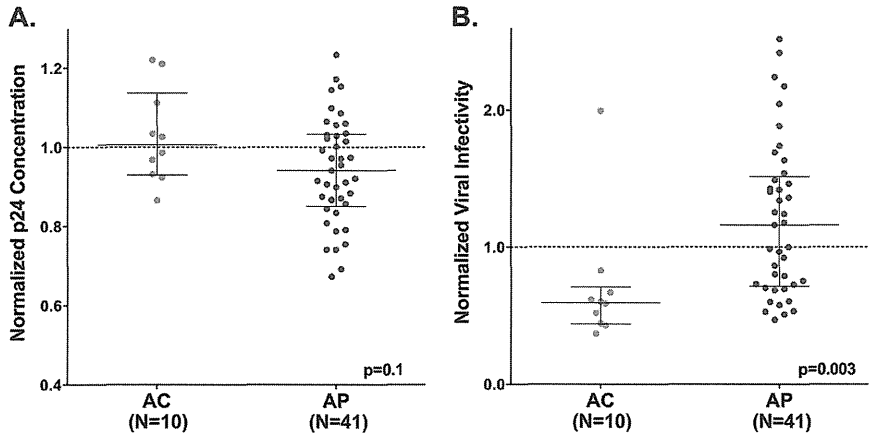

FIG 4 Reduced ability to enhance virion infectivity in AC Nef clones. Plots depict the normalized ability of recombinant viruses encoding representative Nef clones from AC (n = 10, red) and AP (n = 41, blue) to enhance viral production ($p24^{Gag}$ ng/ml) (A) and viral infectivity (B) in Tzm-bl cell assays. A dashed line (---) in each panel illustrates normalized activity of 1.0, which represents the function of positive-control NL4.3-nef_{SF2}. Values below 1.0 indicate lower Nef function relative to NL4.3-nef_{SF2}, while values above 1.0 indicate higher function. Each Nef-containing recombinant virus was tested in duplicate. Note that the negative-control NL4.3Δnef strain displayed a mean infectivity level of 0.02 (standard deviation [SD], 0.009; n = 8 replicates) in this assay.

Changes in Nef activity observed over time in some AC participants. To directly explore changes in Nef function over time in AC, we cloned plasma RNA Nef sequences at a single follow-up time point, collected a median of 283 (IQR, 161 to 427) days after the date of baseline enrollment, from 6 AC individuals from whom a sample was available (Table 1). A median of 4 Nef clones (range, 1 to 11) were isolated per patient at the follow-up time point. CD4 and HLA class I downregulation activities were measured for all unique clones, while a single *nef* allele was used to generate recombinant NL4.3 stocks to assess viral infectivity enhancement (Fig. 5). In a paired analysis comparing the functions of a representative Nef clone from baseline and follow-up samples, we observed no overall differences in the ability of Nef to downregulate CD4 or HLA class I or to enhance viral infectivity (Wilcoxon paired test; all $P > 0.5$). This suggests that Nef functional alterations (whether they be increases or decreases over time) are not generalizable or consistent phenomena during the first year postinfection. However, we did observe substantial changes in these Nef functions in individual cases.

To address this further, we analyzed clonal *nef* sequences from baseline and follow-up time points in 4 AC who displayed the greatest changes in Nef function over time to identify polymorphisms that might contribute to these observations. Notably, in all 4 individuals, most observed sequence changes were linked to an HLA class I allele expressed by the host or to reversion of transmitted viral polymorphisms associated with HLA alleles presumably expressed in previous a host, as defined by reference lists of HLA-associated polymorphisms derived from published statistical association studies (60, 61). For example, selection of 4 polymorphisms associated with HLA-A*31 and B*37 in subject AC01 (discussed below) was accompanied by a 19% reduction in HLA class I downregulation activity, while in subject AC02, reductions in Nef-mediated infectivity enhancement corresponded to the appearance of a B*35-associated polymorphism, H40Q, and reversion to the consensus sequence at D63E (located in the acidic $E_{62}EEE_{65}$ cluster that binds PACS-2 [62]). In AC05, an 18% reduction in CD4 downregulation activity was observed in conjunction with D54E and the B*39-associated N162S polymorphism. Finally, recovery of wild-type HLA class I downregulation function in follow-up clones from AC07 coincided with 10 polymorphisms in the C-terminal half of Nef, the most notable being reversion of a well-characterized A*23/A*24-associated escape

TABLE 2 Correlation analyses for acute controllers (n = 10)[a]

Parameter	Statistic	Baseline pVL	Nef CD4 downregulation	Nef HLA downregulation	Nef infectivity enhancement
Baseline eDPI	R	**−0.77**	−0.52	**−0.85**	0.19
	P	**0.007**	0.1	**0.004**	0.6
Baseline pVL	R		0.48	**0.81**	0.01
	P		0.2	**0.01**	1.0
CD4 downregulation	R			**0.74**	−0.05
	P			**0.02**	0.9
HLA downregulation	R				0.15
	P				0.7

[a] Abbreviations: pVL, plasma viral load; HLA, human leukocyte antigen; eDPI, estimated days postinfection. Data represent Spearman R and *P* values. Significant associations are highlighted in bold type.

TABLE 3 Correlation analyses for acute progressors ($n = 50$)[a]

Parameter	Statistic	Baseline pVL	Nef CD4 downregulation	Nef HLA downregulation	Nef infectivity enhancement
Baseline eDPI	R	**−0.38**	−0.05	0.05	−0.11
	P	**0.007**	0.7	0.8	0.5
Baseline pVL	R		0.17	0.15	**0.54**
	P		0.3	0.3	**<0.001**
CD4 downregulation	R			**0.56**	0.20
	P			**<0.001**	0.2
HLA downregulation	R				−0.10
	P				0.6

[a] Abbreviations: HLA, human leukocyte antigen; eDPI, estimated days postinfection; pVL, plasma viral load. Data represent Spearman R and *P* values; significant associations are highlighted in bold type.

mutation (F135Y) that is reported to alter this activity (63). These results indicate that certain host HLA-associated CTL pressures can select mutations that impact Nef function.

HLA-driven polymorphisms act in combination to reduce Nef function in AC01. AC01 was of particular interest because this subject displayed the greatest reduction in HLA class I downregulation activity and also controlled pVL to less than 50 RNA copies/ml within the first year. Of the 11 clones isolated from this patient at 383 days postinfection, 10 were identical and encoded 4 amino acid polymorphisms (R19K, H40R, M182L, and V194A) that together resulted in a 19% reduction in HLA class I downregulation compared to baseline clone levels (Fig. 6A). The remaining follow-up clone contained a fifth polymorphism (E149K) and displayed 15% and 13% reductions in HLA class I and CD4 downregulation activities, respectively (data not shown). E149 is located at the base of a central loop in Nef (amino acids 149 to 179) that binds to AP-2 (64), suggesting that an E149K charge-reversal mutation may alter interactions with this clathrin adapter complex that are required for CD4 downregulation.

Published HLA-association studies (60, 61) indicate that mutations at Nef residues 19, 40, 182, and 194 are highly significantly associated with HLA-A*31 (codons 19 and 194) and B*37 (Nef codons 40 and 182), two alleles expressed by AC01. R19K is located in a putative A*31-restricted CTL epitope predicted on the basis of this individual's autologous baseline viral sequence (K_9LAGWPTI$\underline{R}_{19}$ [the site of mutation is underlined]; prediction made using NetMHCpan2.8 [65, 66]), while V194A lies within a published A*31-restricted epitope (S_{188}LAFRH$\underline{V}$AR$_{196}$), although the baseline *nef* sequence in AC01 is slightly different (TLAFHH$\underline{V}$AR) (67). Likewise, H40R is found within a published CTL epitope (R_{35}DLEK$\underline{H}$GAI$_{43}$) detected in B*37-expressing vaccine recipients (68), while M182L resides in a predicted A*31-restricted epitope (V_{180}L$\underline{E}$WRFDSR$_{188}$, based on the *nef* consensus sequence) as well as a putative B*37-restricted epitope that is predicted in AC01's baseline viral sequence (K_{178}EVL$\underline{M}$KFDTRL$_{189}$).

Viral adaptation to CTL in early infection commonly involves the appearance of transient polymorphisms in or near the epitope that is under immune pressure, from which the final escape form is ultimately selected (67, 69, 70). Baseline Nef clones from AC01 exhibited polymorphisms near codon 40, notably, D36N and

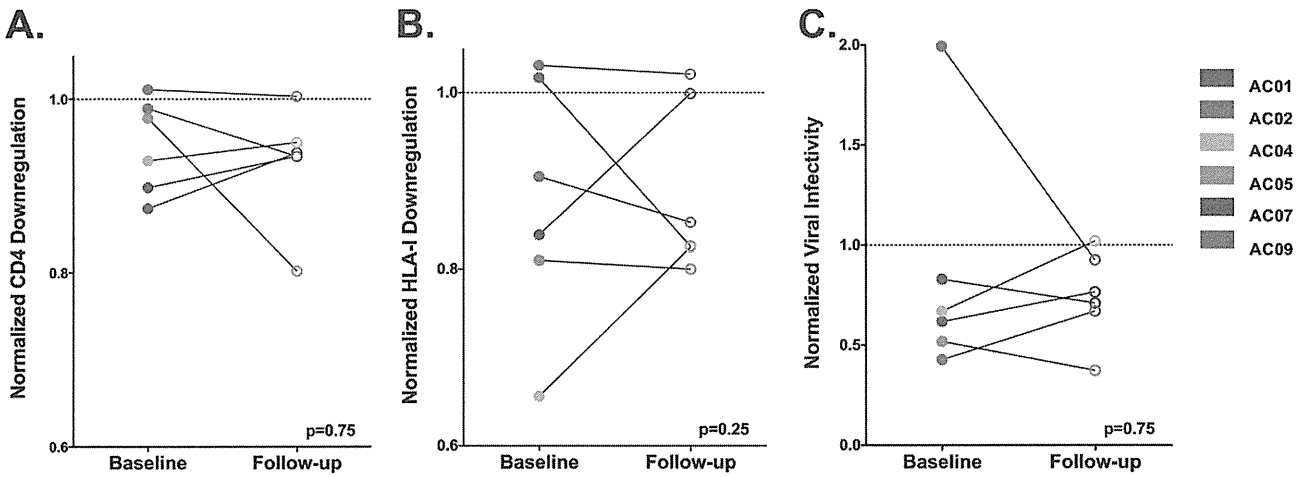

FIG 5 No consistent changes in Nef activity were observed in AC patients over time. The ability of Nef to downregulate CD4 (A) and HLA class I (B) or to enhance viral infectivity (C) is shown for representative clones derived from 6 AC patients at the baseline (closed circles) and follow-up (open circles) time points, as presented in Table 1. A dashed line (---) indicates normalized activity of 1.0, which represents the function of the positive-control Nef_{SF2} in each assay. The Wilcoxon *P* value is shown; no significant differences in Nef function were observed between baseline and follow-up clones in a paired test. Nef downregulation activities were tested in ≥3 replicates, while viral infectivity was tested in duplicate.

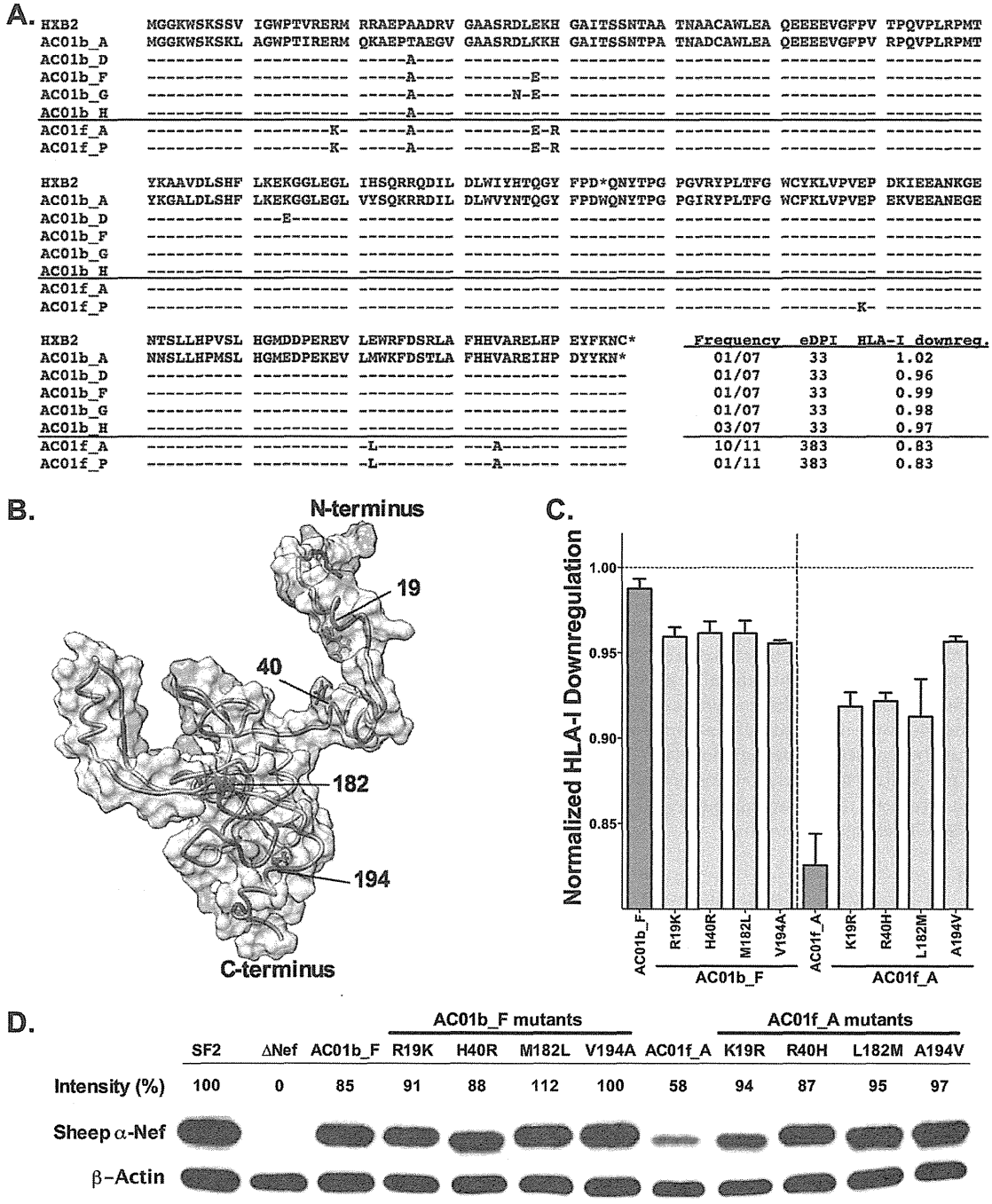

FIG 6 Accumulation of HLA-associated polymorphisms is associated with reduced Nef function and expression. (A) An HXB2 alignment of unique Nef sequences derived from patient AC01 at the baseline ($n = 5$) and follow-up ($n = 2$) time points is shown. Nef_{HXB2} data are indicated for reference. Sequences are labeled by participant identifier (ID) (AC01) followed by the time of sample collection (baseline, b; follow-up, f) and colony identifier (A, B, etc). A solid line distinguishes baseline clones (above the line) from follow-up clones (below the line). Four polymorphisms (R19K, H40R, M182L, and V194A; highlighted in yellow) were observed in all follow-up clones and are associated with host HLA-A*31 or HLA-B*37, as discussed in the text. (B) A model of the Nef protein structure illustrates the location of residues/motifs previously associated with HLA class I downregulation function (green), the four polymorphisms observed in AC01 (red and magenta), and an area of potential overlap near R19 (magenta). (C) A bar graph depicts the normalized HLA class I downregulation activities of baseline clone AC01b_F and follow-up clone AC01f_A (red) and their corresponding single-amino-acid mutants (yellow) at the four polymorphic sites; all samples were tested in ≥4 replicates. A dashed line (---) indicates normalized activity of 1.0, which represents the function of the positive-control Nef_{SF2}. (D) Steady-state protein expression for Nef_{SF2} (positive control), ΔNef (negative control), AC01b_F, and AC01f_A and their corresponding single-amino-acid mutants was examined by Western blotting. β-Actin was used as a cellular protein control. The relative band intensity (%) for each Nef clone was calculated by normalization to β-actin and then Nef_{SF2}. As such, a number > 100% or < 100% represents relative Nef expression greater or less than that of Nef_{SF2}.

E38K, that are consistent with this phenomenon (Fig. 6A). Furthermore, clones isolated at days 51, 65, and 93 encoded D36N, E38G, and K39T (adjacent to the final escape site at codon 40) and H192Y (adjacent to the final escape site at codon 194) (data not shown).

These observations motivated us to undertake a more in-depth analysis of Nef-mediated HLA class I downregulation activity in AC01. Of these 4 polymorphisms, only R19K is located near a residue or motif (namely, M20) that has been associated with this function (Fig. 6B) (58, 63, 71–77). To directly examine their impact on Nef, forward mutations corresponding to each of the 4 polymorphisms were introduced individually into the baseline clone (AC01b_F) whose sequence most closely resembled the B/HXB2 *nef* consensus sequence and backward mutations were introduced into the predominant follow-up clone (AC01f_A) to revert each of these polymorphisms individually. Single-amino-acid changes in the baseline clone had only a modest impact on HLA class I downregulation function (~3% reduction in each case; Fig. 6C). None of the forward mutations altered baseline Nef protein stability appreciably, but each backwards mutation restored expression of the follow-up clone to a level that was comparable to that seen with the baseline sequence (Fig. 6D). Since none of these polymorphisms appeared to have a major effect on Nef function individually, and since Nef expression levels and *in vitro* function could be largely restored by reversion of any one of these mutations alone, our results suggest that all 4 HLA-associated polymorphisms acted in combination to reduce Nef stability, yielding reduced HLA class I downregulation activity in later clones from AC01. In summary, the emergence of HLA-associated mutations that additively impaired Nef function over time in subject AC01 strongly suggests that Nef functional impairment in this individual is not solely attributable to transmission of an attenuated virus but is rather a direct consequence of HLA immunogenetics and $CD8^+$ T cell selection *in vivo*.

DISCUSSION

In this study, we examined *nef* alleles from 10 recently infected individuals who controlled HIV-1 plasma viremia to less than 2,000 RNA copies/ml in the absence of antiretroviral therapy (acute controllers [AC]) and 50 noncontrollers (acute progressors [AP]). While baseline Nef clones from both cohorts were generally functional (all patient-derived clones exhibited activities greater than that of the ΔNef control), those from AC displayed a median of a 5%-reduced ability to downregulate surface CD4, 17%-reduced ability to downregulate HLA class I molecules, and 57% poorer enhancement of virion infectivity compared to those from AP. Although we cannot draw definitive conclusions regarding the clinical significance of these observations, even small changes at the level of each virus-infected cell could be amplified through multiple cycles of infection, thereby influencing pathogenesis.

We previously observed that multiple Nef functions were impaired in chronically HIV-1-infected EC (21), and results presented here demonstrate that similar impairments can be seen at early times postinfection. We therefore conclude that modest functional attenuation of Nef is a relatively common occurrence in individuals who spontaneously control HIV-1. Our results indicate that this may be attributed to transmission of less-fit HIV-1 strains as well as to the acquisition of HLA-associated mutations that compromise Nef function at early times postinfection—and that the precise mechanism may be unique to each individual. Notably, the *in vitro* replication capacity of *gag* and *protease* recombinant viruses is also reduced in this AC cohort through apparently similar means (32). Together, our data support a model where the early function of major HIV-1 structural and accessory proteins has a long-term impact on viremia control and disease progression, which is consistent with studies highlighting the impact of a transmitted/founder viral sequence on clinical outcome (78–80).

In a cross-sectional analysis, baseline HLA class I downregulation function correlated inversely with the baseline sampling date in Nef clones from AC (Table 2). This is consistent with early attenuation of Nef following infection as the transmitted/founder virus adapts to its new host through selection of CTL escape mutations. A similar correlation was not observed for AP (Table 3), suggesting that early changes in Nef sequence in these individuals were not associated with reduced function. Intriguingly, Nef-mediated enhancement of virion infectivity correlated directly with pVL in AP but not in AC; however, additional studies will be necessary to confirm a potential link with this Nef function in the establishment of the viral load set point in HIV-infected persons whose disease progresses normally.

Longitudinal analyses of Nef clones from six AC revealed substantial changes in Nef function in individual patients over time, though neither the direction nor magnitude of these changes was consistent across patients (possibly due to the small number of individuals examined). However, among the four AC who exhibited substantial functional increases or decreases over time, these could be attributed to unique polymorphisms that arose in the first year of infection. Many were consistent with HLA-driven adaptations in the current host or with reversion of HLA-associated polymorphisms present in the baseline sequence; however, only one (F135Y) had been previously described to affect Nef function (63).

Our detailed forward and reverse mutagenesis of clones from AC01 demonstrated that multiple substitutions acted synergistically to affect Nef function in this individual. In particular, four polymorphisms selected by HLA-A*31 and B*37 were required to reduce the ability of Nef to downregulate HLA class I. Together, these results indicate that host CTL pressure can select for escape mutations that directly reduce Nef function over the infection course, indicating that, in at least a subset of controllers, functional impairments are not solely attributable to acquisition of attenuated strains but are rather a direct consequence of HLA-restricted $CD8^+$ T cell selection *in vivo*. Reduced HLA class I downregulation function in follow-up clones from AC01 correlated with lower steady-state Nef protein levels in cells (Fig. 5), and site-directed mutagenesis confirmed that all four HLA-associated polymorphisms were necessary to see both effects. Intriguingly, we observed a 42% reduction in protein levels for the quadruple Nef mutant but only a 19% reduction in its HLA class I downregulation function. This suggests that there may be a threshold effect such that modest reductions in Nef expression are tolerated without a significant loss of function. It is well established that a greater amount of Nef protein is required to promote efficient downregulation of HLA class I (compared to CD4) (81); as such, HLA class I downregulation activity is likely to be more sensitive to alterations in protein expression or stability. Impaired HLA class I downregulation was thus likely due to reduced Nef expression in this case rather than to disruption of a critical functional motif.

Further studies will be necessary to determine if this is a consistent observation for patient-derived Nef clones in other contexts.

Some limitations of this study merit discussion. First, the AC cohort represents a rare group of individuals enrolled during acute/early infection; therefore, the number of individuals and the number of specimens available were limited. When possible, we tested the downregulation activity of multiple Nef clones from each AC, allowing a better assessment of functional diversity within each individual. Similar results for CD4 or HLA class I downregulation were obtained when we analyzed a representative clone, a predominant Nef clone, and the median function of all clones, indicating that our conclusions are not biased by the isolate used. Second, Nef performs multiple roles in virus-infected cells and we have examined only three *in vitro* functions in this study. Our results demonstrate significant impairments in CD4 and HLA class I downregulation function as well as infectivity enhancement for early Nef clones from AC. We have not assessed the ability of Nef to modulate other cellular proteins or functions (including TCR signaling) or potential differences in viral replication capacity using multicycle assays. Further investigation would therefore extend the observations of this study; however, we believe that such work is unlikely to alter our conclusions significantly. Similarly, it has been reported that the effects of Nef on host HLA expression may differ between HLA alleles (82). While we assessed only downregulation of HLA-A*02 here, a previous study by our group observed a strong correlation between the abilities of patient-derived Nef clones to downregulate A*02 and B*07 in this same assay system (56). Changes in Nef function between baseline and follow-up clones sampled were observed up to 516 days later. Thus, it is not clear when these changes occurred. Even in the case of AC01, from whom some intermediate specimens were available, the 4 polymorphisms examined became fixed between days 93 and 383. Finally, even though acute controllers were recruited, on average, less than 2.5 months following their estimated date of infection, we cannot rule out the possibility of very early selection and fixation of immune-driven mutations prior to sampling. Despite these limitations, we believe that the data presented here provide a unique window into early events during natural HIV-1 infection that can help us to better understand the pathways and mechanisms of viral attenuation that may contribute to the controller phenotype.

We conclude that impaired early Nef function is associated with spontaneous control of HIV-1 viremia. This observation is consistent with previous data showing reduced Nef activity in an independent cohort of chronically HIV-1-infected EC (21) and suggests that early functional deficits in Nef—via acquisition of modestly attenuated sequences at transmission or very rapid fixation of host-driven viral mutations—contribute to spontaneous viral control. Importantly, changes in Nef function during the first year postinfection frequently coincided with the appearance or reversion of HLA-associated polymorphisms, indicating that within-host CTL pressures can drive the selection of mutations that modulate Nef activity in at least some individuals. These results highlight the potential for host immune responses to modulate HIV pathogenicity and disease outcome by targeting epitopes in Nef.

ACKNOWLEDGMENTS

This study was supported by the Canadian Institutes for Health Research (CIHR), operating grants MOP-93536 (to Z.L.B.) and THA-118569 (to M.A.B.), and by grants-in-aid from the Global COE Program (Ministry of Education, Science, Sports, and Culture of Japan) and the Ministry of Health, Labor, and Welfare of Japan (to T.U.). X.T.K. is supported by a Master's Scholarship from the Canadian Association for HIV Research in partnership with Bristol-Myers Squibb Canada and ViiV Healthcare. P.M. is supported by Postdoctoral Fellowships from the Michael Smith Foundation for Health Research (MSFHR) and CIHR. A.Q.L. is supported by a CIHR Frederick Banting and Charles Best Masters Award. Z.L.B. is the recipient of a CIHR New Investigator Award and a Scholar Award from MSFHR. M.A.B. holds a Canada Research Chair (Tier 2) in Viral Pathogenesis and Immunity from the Canada Research Chairs Program.

The funders of this study played no role in determining the content of the manuscript or in our decision to publish.

We thank the clinicians, staff, and participants of the Acute Infection Early Disease Research Program (AIEDRP) for their critical contributions to this project. The following reagents were obtained from the NIH AIDS Research and Reference Reagents Program, Division of AIDS, NIAID: TZM-bl, catalog no. 8129, from John C. Kappes, Xiaoyun Wu and Tranzyme Inc.; and HIV-1 Nef antiserum (rabbit), no. 2949, from Ronald Swanstrom. Sheep antiserum to HIV-1 Nef (catalog no. ARP444) was obtained from the Centre for AIDS Reagents, NIBSC (United Kingdom) and was kindly donated by M. Harris.

REFERENCES

1. **Kaslow RA, Carrington M, Apple R, Park L, Munoz A, Saah AJ, Goedert JJ, Winkler C, O'Brien SJ, Rinaldo C, Detels R, Blattner W, Phair J, Erlich H, Mann DL.** 1996. Influence of combinations of human major histocompatibility complex genes on the course of HIV-1 infection. Nat. Med. **2**:405–411. http://dx.doi.org/10.1038/nm0496-405.
2. **Gao X, Nelson GW, Karacki P, Martin MP, Phair J, Kaslow R, Goedert JJ, Buchbinder S, Hoots K, Vlahov D, O'Brien SJ, Carrington M.** 2001. Effect of a single amino acid change in MHC class I molecules on the rate of progression to AIDS. N. Engl. J. Med. **344**:1668–1675. http://dx.doi.org/10.1056/NEJM200105313442203.
3. **International HIV Controllers Study, Pereyra F, Jia X, McLaren PJ, Telenti A, de Bakker PI, Walker BD, Ripke S, Brumme CJ, Pulit SL, Carrington M, Kadie CM, Carlson JM, Heckerman D, Graham RR, Plenge RM, Deeks SG, Gianniny L, Crawford G, Sullivan J, Gonzalez E, Davies L, Camargo A, Moore JM, Beattie N, Gupta S, Crenshaw A, Burtt NP, Guiducci C, Gupta N, Gao X, Qi Y, Yuki Y, Piechocka-Trocha A, Cutrell E, Rosenberg R, Moss KL, Lemay P, O'Leary J, Schaefer T, Verma P, Toth I, Block B, Baker B, Rothchild A, Lian J, Proudfoot J, Alvino DM, Vine S, Addo MM, et al.** 2010. The major genetic determinants of HIV-1 control affect HLA class I peptide presentation. Science **330**:1551–1557. http://dx.doi.org/10.1126/science.1195271.
4. **Fellay J, Shianna KV, Ge D, Colombo S, Ledergerber B, Weale M, Zhang K, Gumbs C, Castagna A, Cossarizza A, Cozzi-Lepri A, De Luca A, Easterbrook P, Francioli P, Mallal S, Martinez-Picado J, Miro JM, Obel N, Smith JP, Wyniger J, Descombes P, Antonarakis SE, Letvin NL, McMichael AJ, Haynes BF, Telenti A, Goldstein DB.** 2007. A whole-genome association study of major determinants for host control of HIV-1. Science **317**:944–947. http://dx.doi.org/10.1126/science.1143767.
5. **McLaren PJ, Coulonges C, Ripke S, van den Berg L, Buchbinder S, Carrington M, Cossarizza A, Dalmau J, Deeks SG, Delaneau O, De Luca A, Goedert JJ, Haas D, Herbeck JT, Kathiresan S, Kirk GD, Lambotte O, Luo M, Mallal S, van Manen D, Martinez-Picado J, Meyer L, Miro JM, Mullins JI, Obel N, O'Brien SJ, Pereyra F, Plummer FA, Poli G, Qi Y, Rucart P, Sandhu MS, Shea PR, Schuitemaker H, Theodorou I, Vannberg F, Veldink J, Walker BD, Weintrob A, Winkler CA, Wolinsky S, Telenti A, Goldstein DB, de Bakker PI, Zagury JF, Fellay J.** 2013. Association study of common genetic variants and HIV-1 acquisition in 6,300 infected cases and 7,200 controls. PLoS Pathog. **9**:e1003515. http://dx.doi.org/10.1371/journal.ppat.1003515.
6. **Pereyra F, Addo MM, Kaufmann DE, Liu Y, Miura T, Rathod A, Baker B, Trocha A, Rosenberg R, Mackey E, Ueda P, Lu Z, Cohen D, Wrin T, Petropoulos CJ, Rosenberg ES, Walker BD.** 2008. Genetic and immunologic heterogeneity among persons who control HIV infection in the absence of therapy. J. Infect. Dis. **197**:563–571. http://dx.doi.org/10.1086/526786.
7. **Deeks SG, Walker BD.** 2007. Human immunodeficiency virus controllers:

mechanisms of durable virus control in the absence of antiretroviral therapy. Immunity 27:406–416. http://dx.doi.org/10.1016/j.immuni.2007.08.010.
8. Migueles SA, Connors M. 2010. Long-term nonprogressive disease among untreated HIV-infected individuals: clinical implications of understanding immune control of HIV. JAMA 304:194–201. http://dx.doi.org/10.1001/jama.2010.925.
9. Ndhlovu ZM, Proudfoot J, Cesa K, Alvino DM, McMullen A, Vine S, Stampouloglou E, Piechocka-Trocha A, Walker BD, Pereyra F. 2012. Elite controllers with low to absent effector CD8+ T cell responses maintain highly functional, broadly directed central memory responses. J. Virol. 86:6959–6969. http://dx.doi.org/10.1128/JVI.00531-12.
10. Hersperger AR, Pereyra F, Nason M, Demers K, Sheth P, Shin LY, Kovacs CM, Rodriguez B, Sieg SF, Teixeira-Johnson L, Gudonis D, Goepfert PA, Lederman MM, Frank I, Makedonas G, Kaul R, Walker BD, Betts MR. 2010. Perforin expression directly ex vivo by HIV-specific CD8 T-cells is a correlate of HIV elite control. PLoS Pathog. 6:e1000917. http://dx.doi.org/10.1371/journal.ppat.1000917.
11. Migueles SA, Laborico AC, Shupert WL, Sabbaghian MS, Rabin R, Hallahan CW, Van Baarle D, Kostense S, Miedema F, McLaughlin M, Ehler L, Metcalf J, Liu S, Connors M. 2002. HIV-specific CD8+ T cell proliferation is coupled to perforin expression and is maintained in nonprogressors. Nat. Immunol. 3:1061–1068. http://dx.doi.org/10.1038/ni845.
12. Hersperger AR, Migueles SA, Betts MR, Connors M. 2011. Qualitative features of the HIV-specific CD8+ T-cell response associated with immunologic control. Curr. Opin. HIV AIDS 6:169–173. http://dx.doi.org/10.1097/COH.0b013e3283454c39.
13. Kiepiela P, Ngumbela K, Thobakgale C, Ramduth D, Honeyborne I, Moodley E, Reddy S, de Pierres C, Mncube Z, Mkhwanazi N, Bishop K, van der Stok M, Nair K, Khan N, Crawford H, Payne R, Leslie A, Prado J, Prendergast A, Frater J, McCarthy N, Brander C, Learn GH, Nickle D, Rousseau C, Coovadia H, Mullins JI, Heckerman D, Walker BD, Goulder P. 2007. CD8+ T-cell responses to different HIV proteins have discordant associations with viral load. Nat. Med. 13:46–53. http://dx.doi.org/10.1038/nm1520.
14. Adland E, Carlson JM, Paioni P, Kloverpris H, Shapiro R, Ogwu A, Riddell L, Luzzi G, Chen F, Balachandran T, Heckerman D, Stryhn A, Edwards A, Ndung'u T, Walker BD, Buus S, Goulder P, Matthews PC. 2013. Nef-specific CD8+ T cell responses contribute to HIV-1 immune control. PLoS One 8:e73117. http://dx.doi.org/10.1371/journal.pone.0073117.
15. Riou C, Burgers WA, Mlisana K, Koup RA, Roederer M, Abdool Karim SS, Williamson C, Gray CM. 2014. Differential impact of magnitude, polyfunctional capacity, and specificity of HIV-specific CD8+ T cell responses on HIV set point. J. Virol. 88:1819–1824. http://dx.doi.org/10.1128/JVI.02968-13.
16. Allen TM, Altfeld M. 2008. Crippling HIV one mutation at a time. J. Exp. Med. 205:1003–1007. http://dx.doi.org/10.1084/jem.20080569.
17. Prince JL, Claiborne DT, Carlson JM, Schaefer M, Yu T, Lahki S, Prentice HA, Yue L, Vishwanathan SA, Kilembe W, Goepfert P, Price MA, Gilmour J, Mulenga J, Farmer P, Derdeyn CA, Tang J, Heckerman D, Kaslow RA, Allen SA, Hunter E. 2012. Role of transmitted Gag CTL polymorphisms in defining replicative capacity and early HIV-1 pathogenesis. PLoS Pathog. 8:e1003041. http://dx.doi.org/10.1371/journal.ppat.1003041.
18. Brumme ZL, Li C, Miura T, Sela J, Rosato PC, Brumme CJ, Markle TJ, Martin E, Block BL, Trocha A, Kadie CM, Allen TM, Pereyra F, Heckerman D, Walker BD, Brockman MA. 2011. Reduced replication capacity of NL4-3 recombinant viruses encoding reverse transcriptase-integrase sequences from HIV-1 elite controllers. J. Acquir. Immune Defic. Syndr. 56:100–108. http://dx.doi.org/10.1097/QAI.0b013e3181fe9450.
19. Lassen KG, Lobritz MA, Bailey JR, Johnston S, Nguyen S, Lee B, Chou T, Siliciano RF, Markowitz M, Arts EJ. 2009. Elite suppressor-derived HIV-1 envelope glycoproteins exhibit reduced entry efficiency and kinetics. PLoS Pathog. 5:e1000377. http://dx.doi.org/10.1371/journal.ppat.1000377.
20. Miura T, Brockman MA, Brumme ZL, Brumme CJ, Pereyra F, Trocha A, Block BL, Schneidewind A, Allen TM, Heckerman D, Walker BD. 2009. HLA-associated alterations in replication capacity of chimeric NL4-3 viruses carrying gag-protease from elite controllers of human immunodeficiency virus type 1. J. Virol. 83:140–149. http://dx.doi.org/10.1128/JVI.01471-08.
21. Mwimanzi P, Markle TJ, Martin E, Ogata Y, Kuang XT, Tokunaga M, Mahiti M, Pereyra F, Miura T, Walker BD, Brumme ZL, Brockman MA, Ueno T. 2013. Attenuation of multiple Nef functions in HIV-1 elite controllers. Retrovirology 10:1. http://dx.doi.org/10.1186/1742-4690-10-1.
22. Lobritz MA, Lassen KG, Arts EJ. 2011. HIV-1 replicative fitness in elite controllers. Curr. Opin. HIV AIDS 6:214–220. http://dx.doi.org/10.1097/COH.0b013e3283454cf5.
23. Rihn SJ, Wilson SJ, Loman NJ, Alim M, Bakker SE, Bhella D, Gifford RJ, Rixon FJ, Bieniasz PD. 2013. Extreme genetic fragility of the HIV-1 capsid. PLoS Pathog. 9:e1003461. http://dx.doi.org/10.1371/journal.ppat.1003461.
24. Crawford H, Prado JG, Leslie A, Hue S, Honeyborne I, Reddy S, van der Stok M, Mncube Z, Brander C, Rousseau C, Mullins JI, Kaslow R, Goepfert P, Allen S, Hunter E, Mulenga J, Kiepiela P, Walker BD, Goulder PJ. 2007. Compensatory mutation partially restores fitness and delays reversion of escape mutation within the immunodominant HLA-B*5703-restricted Gag epitope in chronic human immunodeficiency virus type 1 infection. J. Virol. 81:8346–8351. http://dx.doi.org/10.1128/JVI.00465-07.
25. Martinez-Picado J, Prado JG, Fry EE, Pfafferott K, Leslie A, Chetty S, Thobakgale C, Honeyborne I, Crawford H, Matthews P, Pillay T, Rousseau C, Mullins JI, Brander C, Walker BD, Stuart DI, Kiepiela P, Goulder P. 2006. Fitness cost of escape mutations in p24 Gag in association with control of human immunodeficiency virus type 1. J. Virol. 80:3617–3623. http://dx.doi.org/10.1128/JVI.80.7.3617-3623.2006.
26. Brockman MA, Schneidewind A, Lahaie M, Schmidt A, Miura T, Desouza I, Ryvkin F, Derdeyn CA, Allen S, Hunter E, Mulenga J, Goepfert PA, Walker BD, Allen TM. 2007. Escape and compensation from early HLA-B57-mediated cytotoxic T-lymphocyte pressure on human immunodeficiency virus type 1 Gag alter capsid interactions with cyclophilin A. J. Virol. 81:12608–12618. http://dx.doi.org/10.1128/JVI.01369-07.
27. Rolland M, Manocheewa S, Swain JV, Lanxon-Cookson EC, Kim M, Westfall DH, Larsen BB, Gilbert PB, Mullins JI. 2013. HIV-1 conserved-element vaccines: relationship between sequence conservation and replicative capacity. J. Virol. 87:5461–5467. http://dx.doi.org/10.1128/JVI.03033-12.
28. Brockman MA, Brumme ZL, Brumme CJ, Miura T, Sela J, Rosato PC, Kadie CM, Carlson JM, Markle TJ, Streeck H, Kelleher AD, Markowitz M, Jessen H, Rosenberg E, Altfeld M, Harrigan PR, Heckerman D, Walker BD, Allen TM. 2010. Early selection in Gag by protective HLA alleles contributes to reduced HIV-1 replication capacity that may be largely compensated for in chronic infection. J. Virol. 84:11937–11949. http://dx.doi.org/10.1128/JVI.01086-10.
29. Brockman MA, Chopera DR, Olvera A, Brumme CJ, Sela J, Markle TJ, Martin E, Carlson JM, Le AQ, McGovern R, Cheung PK, Kelleher AD, Jessen H, Markowitz M, Rosenberg E, Frahm N, Sanchez J, Mallal S, John M, Harrigan PR, Heckerman D, Brander C, Walker BD, Brumme ZL. 2012. Uncommon pathways of immune escape attenuate HIV-1 integrase replication capacity. J. Virol. 86:6913–6923. http://dx.doi.org/10.1128/JVI.07133-11.
30. Troyer RM, McNevin J, Liu Y, Zhang SC, Krizan RW, Abraha A, Tebit DM, Zhao H, Avila S, Lobritz MA, McElrath MJ, Le Gall S, Mullins JI, Arts EJ. 2009. Variable fitness impact of HIV-1 escape mutations to cytotoxic T lymphocyte (CTL) response. PLoS Pathog. 5:e1000365. http://dx.doi.org/10.1371/journal.ppat.1000365.
31. Miura T, Brumme CJ, Brockman MA, Brumme ZL, Pereyra F, Block BL, Trocha A, John M, Mallal S, Harrigan PR, Walker BD. 2009. HLA-associated viral mutations are common in human immunodeficiency virus type 1 elite controllers. J. Virol. 83:3407–3412. http://dx.doi.org/10.1128/JVI.02459-08.
32. Miura T, Brumme ZL, Brockman MA, Rosato P, Sela J, Brumme CJ, Pereyra F, Kaufmann DE, Trocha A, Block BL, Daar ES, Connick E, Jessen H, Kelleher AD, Rosenberg E, Markowitz M, Schafer K, Vaida F, Iwamoto A, Little S, Walker BD. 2010. Impaired replication capacity of acute/early viruses in persons who become HIV controllers. J. Virol. 84:7581–7591. http://dx.doi.org/10.1128/JVI.00286-10.
33. Mwimanzi P, Markle TJ, Ueno T, Brockman MA. 2012. Human leukocyte antigen (HLA) class I down-regulation by human immunodeficiency virus type 1 negative factor (HIV-1 Nef): what might we learn from natural sequence variants? Viruses 4:1711–1730. http://dx.doi.org/10.3390/v4091711.
34. Garcia JV, Miller AD. 1991. Serine phosphorylation-independent down-regulation of cell-surface CD4 by nef. Nature 350:508–511. http://dx.doi.org/10.1038/350508a0.

35. Schwartz O, Marechal V, Le Gall S, Lemonnier F, Heard JM. 1996. Endocytosis of major histocompatibility complex class I molecules is induced by the HIV-1 Nef protein. Nat. Med. 2:338–342. http://dx.doi.org/10.1038/nm0396-338.
36. Schindler M, Wurfl S, Benaroch P, Greenough TC, Daniels R, Easterbrook P, Brenner M, Munch J, Kirchhoff F. 2003. Down-modulation of mature major histocompatibility complex class II and up-regulation of invariant chain cell surface expression are well-conserved functions of human and simian immunodeficiency virus nef alleles. J. Virol. 77:10548–10556. http://dx.doi.org/10.1128/JVI.77.19.10548-10556.2003.
37. Münch J, Rajan D, Schindler M, Specht A, Rücker E, Novembre FJ, Nerrienet E, Müller-Trutwin MC, Peeters M, Hahn BH, Kirchhoff F. 2007. Nef-mediated enhancement of virion infectivity and stimulation of viral replication are fundamental properties of primate lentiviruses. J. Virol. 81:13852–13864. http://dx.doi.org/10.1128/JVI.00904-07.
38. Miller MD, Warmerdam MT, Gaston I, Greene WC, Feinberg MB. 1994. The human immunodeficiency virus-1 nef gene product: a positive factor for viral infection and replication in primary lymphocytes and macrophages. J. Exp. Med. 179:101–113. http://dx.doi.org/10.1084/jem.179.1.101.
39. Abraham L, Fackler OT. 2012. HIV-1 Nef: a multifaceted modulator of T cell receptor signaling. Cell Commun. Signal. 10:39. http://dx.doi.org/10.1186/1478-811X-10-39.
40. Markle TJ, Philip M, Brockman MA. 2013. HIV-1 Nef and T-cell activation: a history of contradictions. Future Virol. 2013:8. http://dx.doi.org/10.2217/fvl.13.20.
41. Daniel MD, Kirchhoff F, Czajak SC, Sehgal PK, Desrosiers RC. 1992. Protective effects of a live attenuated SIV vaccine with a deletion in the *nef* gene. Science 258:1938–1941. http://dx.doi.org/10.1126/science.1470917.
42. Deacon NJ, Tsykin A, Solomon A, Smith K, Ludford-Menting M, Hooker DJ, McPhee DA, Greenway AL, Ellett A, Chatfield C, Lawson VA, Crowe S, Maerz A, Sonza S, Learmont J, Sullivan JS, Cunningham A, Dwyer D, Dowton D, Mills J. 1995. Genomic structure of an attenuated quasi species of HIV-1 from a blood transfusion donor and recipients. Science 270:988–991. http://dx.doi.org/10.1126/science.270.5238.988.
43. Kirchhoff F, Greenough TC, Brettler DB, Sullivan JL, Desrosiers RC. 1995. Brief report: absence of intact nef sequences in a long-term survivor with nonprogressive HIV-1 infection. N. Engl. J. Med. 332:228–232. http://dx.doi.org/10.1056/NEJM199501263320405.
44. Zaunders JJ, Geczy AF, Dyer WB, McIntyre LB, Cooley MA, Ashton LJ, Raynes-Greenow CH, Learmont J, Cooper DA, Sullivan JS. 1999. Effect of long-term infection with nef-defective attenuated HIV type 1 on CD4+ and CD8+ T lymphocytes: increased CD45RO+CD4+ T lymphocytes and limited activation of CD8+ T lymphocytes. AIDS Res. Hum. Retroviruses 15:1519–1527. http://dx.doi.org/10.1089/088922299309801.
45. Little SJ, Frost SD, Wong JK, Smith DM, Pond SL, Ignacio CC, Parkin NT, Petropoulos CJ, Richman DD. 2008. Persistence of transmitted drug resistance among subjects with primary human immunodeficiency virus infection. J. Virol. 82:5510–5518. http://dx.doi.org/10.1128/JVI.02579-07.
46. Woods CK, Brumme CJ, Liu TF, Chui CK, Chu AL, Wynhoven B, Hall TA, Trevino C, Shafer RW, Harrigan PR. 2012. Automating HIV drug resistance genotyping with RECall, a freely accessible sequence analysis tool. J. Clin. Microbiol. 50:1936–1942. http://dx.doi.org/10.1128/JCM.06689-11.
47. Pond SL, Frost SD, Muse SV. 2005. HyPhy: hypothesis testing using phylogenies. Bioinformatics 21:676–679. http://dx.doi.org/10.1093/bioinformatics/bti079.
48. Guindon S, Gascuel O. 2003. A simple, fast, and accurate algorithm to estimate large phylogenies by maximum likelihood. Syst. Biol. 52:696–704. http://dx.doi.org/10.1080/10635150390235520.
49. Guindon S, Dufayard JF, Lefort V, Anisimova M, Hordijk W, Gascuel O. 2010. New algorithms and methods to estimate maximum-likelihood phylogenies: assessing the performance of PhyML 3.0. Syst. Biol. 59:307–321. http://dx.doi.org/10.1093/sysbio/syq010.
50. Cotton LA, Abdur Rahman M, Ng C, Le AQ, Milloy MJ, Mo T, Brumme ZL. 2012. HLA class I sequence-based typing using DNA recovered from frozen plasma. J. Immunol. Methods 382:40–47. http://dx.doi.org/10.1016/j.jim.2012.05.003.
51. Ueno T, Motozono C, Dohki S, Mwimanzi P, Rauch S, Fackler OT, Oka S, Takiguchi M. 2008. CTL-mediated selective pressure influences dynamic evolution and pathogenic functions of HIV-1 Nef. J. Immunol. 180:1107–1116. http://dx.doi.org/10.4049/jimmunol.180.2.1107.
52. Mwimanzi P, Hasan Z, Hassan R, Suzu S, Takiguchi M, Ueno T. 2011. Effects of naturally-arising HIV Nef mutations on cytotoxic T lymphocyte recognition and Nef's functionality in primary macrophages. Retrovirology 8:50. http://dx.doi.org/10.1186/1742-4690-8-50.
53. Wei X, Decker JM, Liu H, Zhang Z, Arani RB, Kilby JM, Saag MS, Wu X, Shaw GM, Kappes JC. 2002. Emergence of resistant human immunodeficiency virus type 1 in patients receiving fusion inhibitor (T-20) monotherapy. Antimicrob. Agents Chemother. 46:1896–1905. http://dx.doi.org/10.1128/AAC.46.6.1896-1905.2002.
54. Shugars DC, Smith MS, Glueck DH, Nantermet PV, Seillier-Moiseiwitsch F, Swanstrom R. 1993. Analysis of human immunodeficiency virus type 1 nef gene sequences present in vivo. J. Virol. 67:4639–4650.
55. Ho SN, Hunt HD, Horton RM, Pullen JK, Pease LR. 1989. Site-directed mutagenesis by overlap extension using the polymerase chain reaction. Gene 77:51–59. http://dx.doi.org/10.1016/0378-1119(89)90358-2.
56. Mann JK, Byakwaga H, Kuang XT, Le AQ, Brumme CJ, Mwimanzi P, Omarjee S, Martin E, Lee GQ, Baraki B, Danroth R, McCloskey R, Muzoora C, Bangsberg DR, Hunt PW, Goulder PJ, Walker BD, Harrigan PR, Martin JN, Ndung'u T, Brockman MA, Brumme ZL. 2013. Ability of HIV-1 Nef to downregulate CD4 and HLA class I differs among viral subtypes. Retrovirology 10:100. http://dx.doi.org/10.1186/1742-4690-10-100.
57. Mwimanzi P, Markle TJ, Ogata Y, Martin E, Tokunaga M, Mahiti M, Kuang XT, Walker BD, Brockman MA, Brumme ZL, Ueno T. 2013. Dynamic range of Nef functions in chronic HIV-1 infection. Virology 439:74–80. http://dx.doi.org/10.1016/j.virol.2013.02.005.
58. Foster JL, Denial SJ, Temple BR, Garcia JV. 2011. Mechanisms of HIV-1 Nef function and intracellular signaling. J. Neuroimmune Pharmacol. 6:230–246. http://dx.doi.org/10.1007/s11481-011-9262-y.
59. Landi A, Iannucci V, Nuffel AV, Meuwissen P, Verhasselt B. 2011. One protein to rule them all: modulation of cell surface receptors and molecules by HIV Nef. Curr. HIV Res. 9:496–504. http://dx.doi.org/10.2174/157016211798842116.
60. Brumme ZL, Brumme CJ, Chui C, Mo T, Wynhoven B, Woods CK, Henrick BM, Hogg RS, Montaner JS, Harrigan PR. 2007. Effects of human leukocyte antigen class I genetic parameters on clinical outcomes and survival after initiation of highly active antiretroviral therapy. J. Infect. Dis. 195:1694–1704. http://dx.doi.org/10.1086/516789.
61. Brumme ZL, John M, Carlson JM, Brumme CJ, Chan D, Brockman MA, Swenson LC, Tao I, Szeto S, Rosato P, Sela J, Kadie CM, Frahm N, Brander C, Haas DW, Riddler SA, Haubrich R, Walker BD, Harrigan PR, Heckerman D, Mallal S. 2009. HLA-associated immune escape pathways in HIV-1 subtype B Gag, Pol and Nef proteins. PLoS One 4:e6687. http://dx.doi.org/10.1371/journal.pone.0006687.
62. Atkins KM, Thomas L, Youker RT, Harriff MJ, Pissani F, You H, Thomas G. 2008. HIV-1 Nef binds PACS-2 to assemble a multikinase cascade that triggers major histocompatibility complex class I (MHC-I) down-regulation: analysis using short interfering RNA and knock-out mice. J. Biol. Chem. 283:11772–11784. http://dx.doi.org/10.1074/jbc.M707572200.
63. Lewis MJ, Lee P, Ng HL, Yang OO. 2012. Immune selection in vitro reveals human immunodeficiency virus type 1 Nef sequence motifs important for its immune evasion function in vivo. J. Virol. 86:7126–7135. http://dx.doi.org/10.1128/JVI.00878-12.
64. Ren X, Park SY, Bonifacino JS, Hurley JH. 2014. How HIV-1 Nef hijacks the AP-2 clathrin adaptor to downregulate CD4. eLife 3:e01754. http://dx.doi.org/10.7554/eLife.01754.
65. Hoof I, Peters B, Sidney J, Pedersen LE, Sette A, Lund O, Buus S, Nielsen M. 2009. NetMHCpan, a method for MHC class I binding prediction beyond humans. Immunogenetics 61:1–13. http://dx.doi.org/10.1007/s00251-008-0341-z.
66. Nielsen M, Lundegaard C, Blicher T, Lamberth K, Harndahl M, Justesen S, Roder G, Peters B, Sette A, Lund O, Buus S. 2007. NetMHCpan, a method for quantitative predictions of peptide binding to any HLA-A and -B locus protein of known sequence. PLoS One 2:e796. http://dx.doi.org/10.1371/journal.pone.0000796.
67. Goonetilleke N, Liu MK, Salazar-Gonzalez JF, Ferrari G, Giorgi E, Ganusov VV, Keele BF, Learn GH, Turnbull EL, Salazar MG, Weinhold KJ, Moore S, CHAVI Clinical Core B, Letvin N, Haynes BF, Cohen MS, Hraber P, Bhattacharya T, Borrow P, Perelson AS, Hahn BH, Shaw GM, Korber BT, McMichael AJ. 2009. The first T cell response to transmitted/founder virus contributes to the control of acute viremia in HIV-1 infection. J. Exp. Med. 206:1253–1272. http://dx.doi.org/10.1084/jem.20090365.

68. Li F, Finnefrock AC, Dubey SA, Korber BT, Szinger J, Cole S, McElrath MJ, Shiver JW, Casimiro DR, Corey L, Self SG. 2011. Mapping HIV-1 vaccine induced T-cell responses: bias towards less-conserved regions and potential impact on vaccine efficacy in the Step study. PLoS One 6:e20479. http://dx.doi.org/10.1371/journal.pone.0020479.
69. Fischer W, Ganusov VV, Giorgi EE, Hraber PT, Keele BF, Leitner T, Han CS, Gleasner CD, Green L, Lo CC, Nag A, Wallstrom TC, Wang S, McMichael AJ, Haynes BF, Hahn BH, Perelson AS, Borrow P, Shaw GM, Bhattacharya T, Korber BT. 2010. Transmission of single HIV-1 genomes and dynamics of early immune escape revealed by ultra-deep sequencing. PLoS One 5:e12303. http://dx.doi.org/10.1371/journal.pone.0012303.
70. Henn MR, Boutwell CL, Charlebois P, Lennon NJ, Power KA, Macalalad AR, Berlin AM, Malboeuf CM, Ryan EM, Gnerre S, Zody MC, Erlich RL, Green LM, Berical A, Wang Y, Casali M, Streeck H, Bloom AK, Dudek T, Tully D, Newman R, Axten KL, Gladden AD, Battis L, Kemper M, Zeng Q, Shea TP, Gujja S, Zedlack C, Gasser O, Brander C, Hess C, Gunthard HF, Brumme ZL, Brumme CJ, Bazner S, Rychert J, Tinsley JP, Mayer KH, Rosenberg E, Pereyra F, Levin JZ, Young SK, Jessen H, Altfeld M, Birren BW, Walker BD, Allen TM. 2012. Whole genome deep sequencing of HIV-1 reveals the impact of early minor variants upon immune recognition during acute infection. PLoS Pathog. 8:e1002529. http://dx.doi.org/10.1371/journal.ppat.1002529.
71. Akari H, Arold S, Fukumori T, Okazaki T, Strebel K, Adachi A. 2000. Nef-induced major histocompatibility complex class I down-regulation is functionally dissociated from its virion incorporation, enhancement of viral infectivity, and CD4 down-regulation. J. Virol. 74:2907–2912. http://dx.doi.org/10.1128/JVI.74.6.2907-2912.2000.
72. Geyer M, Fackler OT, Peterlin BM. 2001. Structure-function relationships in HIV-1 Nef. EMBO Rep. 2:580–585. http://dx.doi.org/10.1093/embo-reports/kve141.
73. Jia X, Singh R, Homann S, Yang H, Guatelli J, Xiong Y. 2012. Structural basis of evasion of cellular adaptive immunity by HIV-1 Nef. Nat. Struct. Mol. Biol. 19:701–706. http://dx.doi.org/10.1038/nsmb.2328.
74. Kuo LS, Baugh LL, Denial SJ, Watkins RL, Liu M, Garcia JV, Foster JL. 2012. Overlapping effector interfaces define the multiple functions of the HIV-1 Nef polyproline helix. Retrovirology 9:47. http://dx.doi.org/10.1186/1742-4690-9-47.
75. Mangasarian A, Piguet V, Wang JK, Chen YL, Trono D. 1999. Nef-induced CD4 and major histocompatibility complex class I (MHC-I) down-regulation are governed by distinct determinants: N-terminal alpha helix and proline repeat of Nef selectively regulate MHC-I trafficking. J. Virol. 73:1964–1973.
76. Schaefer MR, Wonderlich ER, Roeth JF, Leonard JA, Collins KL. 2008. HIV-1 Nef targets MHC-I and CD4 for degradation via a final common beta-COP-dependent pathway in T cells. PLoS Pathog. 4:e1000131. http://dx.doi.org/10.1371/journal.ppat.1000131.
77. Yamada T, Kaji N, Odawara T, Chiba J, Iwamoto A, Kitamura Y. 2003. Proline 78 is crucial for human immunodeficiency virus type 1 Nef to down-regulate class I human leukocyte antigen. J. Virol. 77:1589–1594. http://dx.doi.org/10.1128/JVI.77.2.1589-1594.2003.
78. Chopera DR, Woodman Z, Mlisana K, Mlotshwa M, Martin DP, Seoighe C, Treurnicht F, de Rosa DA, Hide W, Karim SA, Gray CM, Williamson C, Team CS. 2008. Transmission of HIV-1 CTL escape variants provides HLA-mismatched recipients with a survival advantage. PLoS Pathog. 4:e1000033. http://dx.doi.org/10.1371/journal.ppat.1000033.
79. Goepfert PA, Lumm W, Farmer P, Matthews P, Prendergast A, Carlson JM, Derdeyn CA, Tang J, Kaslow RA, Bansal A, Yusim K, Heckerman D, Mulenga J, Allen S, Goulder PJ, Hunter E. 2008. Transmission of HIV-1 Gag immune escape mutations is associated with reduced viral load in linked recipients. J. Exp. Med. 205:1009–1017. http://dx.doi.org/10.1084/jem.20072457.
80. Fraser C, Lythgoe K, Leventhal GE, Shirreff G, Hollingsworth TD, Alizon S, Bonhoeffer S. 2014. Virulence and pathogenesis of HIV-1 infection: an evolutionary perspective. Science 343:1243727. http://dx.doi.org/10.1126/science.1243727.
81. Liu X, Schrager JA, Lange GD, Marsh JW. 2001. HIV Nef-mediated cellular phenotypes are differentially expressed as a function of intracellular Nef concentrations. J. Biol. Chem. 276:32763–32770. http://dx.doi.org/10.1074/jbc.M101025200.
82. Rajapaksa US, Li D, Peng YC, McMichael AJ, Dong T, Xu XN. 2012. HLA-B may be more protective against HIV-1 than HLA-A because it resists negative regulatory factor (Nef) mediated down-regulation. Proc. Natl. Acad. Sci. U. S. A. 109:13353–13358. http://dx.doi.org/10.1073/pnas.1204199109.

Virus Research 195 (2015) 25–34

Contents lists available at ScienceDirect

Virus Research

journal homepage: www.elsevier.com/locate/virusres

The HIV-1 accessory protein Vpr induces the degradation of the anti-HIV-1 agent APOBEC3G through a VprBP-mediated proteasomal pathway

Dawei Zhou[a], Yan Wang[a], Kenzo Tokunaga[b], Fang Huang[a], Binlian Sun[a,*], Rongge Yang[a,*]

[a] Research Group of HIV Molecular Epidemiology and Virology, Center for Emerging Infectious Diseases, The State Key Laboratory of Virology, Wuhan Institute of Virology, Chinese Academy of Sciences, Wuhan, Hubei 430071, PR China
[b] Department of Pathology, National Institute of Infectious Diseases, 1-23-1 Toyama, Shinjuku-ku, Tokyo 162-8640, Japan

ARTICLE INFO

Article history:
Received 3 June 2014
Received in revised form 28 August 2014
Accepted 28 August 2014
Available online 6 September 2014

Keywords:
HIV-1
Vpr
APOBEC3G (A3G)
Encapsidation
VprBP
Degradation

ABSTRACT

The host anti-HIV-1 factor APOBEC3G (A3G) plays a potential role in restricting HIV-1 replication, although this antagonist can be encountered and disarmed by the Vif protein. In this paper, we report that another HIV-1 accessory protein, viral protein R (Vpr), can interact with A3G and intervene in its antiviral behavior. The interaction of Vpr and A3G was predicted by computer-based screen and confirmed by a co-immunoprecipitation (Co-IP) approach. We found that Vpr could reduce the virion encapsidation of A3G to enhance viral replication. Subsequent experiments showed that Vpr downregulated A3G through Vpr-binding protein (VprBP)-mediated proteasomal degradation, and further confirmed that the reduction of A3G encapsidation associated with Vpr was due to Vpr's degradation-inducing activity. Our findings highlight the versatility of Vpr by unveiling the hostile relationship between Vpr and A3G. In addition, the observation that A3G is targeted to the proteasomal degradation pathway by Vpr in addition to Vif implicates the existence of crosstalk between different HIV-1-host ubiquitin ligase complex systems.

1. Introduction

Viral protein R (Vpr), a virion-associated accessory protein composed of 96 amino acids, is an indispensable factor for efficacious infection and the pathogenesis of HIV-1 (Kogan and Rappaport, 2011). Vpr is highly conserved in HIV-1, HIV-2 and SIV, but a homologous protein, Vpx, is not found in HIV-1 (Tristem et al., 1992). Early studies of Vpr as a pathogenetic factor reported delayed AIDS progression and a low viral titer in peripheral blood from monkeys infected with Vpr-deficient SIV (Hoch et al., 1995; Lang et al., 1993). Since that study, numerous functions of Vpr in aiding the life cycle and pathogenesis of HIV-1 have been reported, including an ability to induce G2-phase arrest during cell division, import of the pre-integration complex (PIC) into the nucleus, regulation of apoptosis, transactivation of viral and cellular genes and modulation of cell signaling (Le Rouzic and Benichou, 2005). Moreover, increasing numbers of host proteins that can interact with Vpr have been identified, but the mechanisms of these interactions remain elusive (Zhao et al., 2011).

One of the most exciting functions of Vpr that has recently attracted attention is its ability to bind to the E3 ubiquitin ligase complex (Romani and Cohen, 2012), which may form a bridge with the proteasome to induce the degradation of a variety of substrates. This widespread phenomenon is a vital regulatory mode of cells that triggers diverse downstream effects. Vpr-binding protein (VprBP), also known as DDB1-Cul4A associated factor 1 (DCAF1), is the key adaptor allowing Vpr to recruit this type of complex. Many substrates have been reported, such as the DNA repair enzymes uracil DNA glycosylase 2 (UNG2) and single-strand-selective monofunctional uracil-DNA glycosylase 1 (SMUG1) (Schrofelbauer et al., 2005), the type I interferon (IFN) inducer IFN regulatory factor 3 (IRF-3) (Okumura et al., 2008), a catalytic subunit of telomerase named TERT (Wang et al., 2013), the RNA-induced silencing complex (RISC) promoter Dicer (Klockow et al., 2013), and the transcriptional regulators ZIP and sZIP (Maudet et al., 2013). Intriguingly, it is well accepted that Vpr's property of arresting the cell cycle at G2-phase is most likely dependent on the degradation of an unknown essential factor (DeHart and Planelles, 2008).

* Corresponding authors. Tel.: +86 27 87198736; fax: +86 27 87198736.
E-mail addresses: sunbl@wh.iov.cn (B. Sun), ryang@wh.iov.cn (R. Yang).

http://dx.doi.org/10.1016/j.virusres.2014.08.021
0168-1702/

The effective replication of HIV-1 in host cells can be limited at nearly every step by several cellular restriction factors, among which APOBEC3G (A3G) has recently been extensively investigated. A3G, first identified in 2002 (Sheehy et al., 2002), belongs to the APOBEC family, possessing cytidine deaminase activity, and is the member of this family with the most potential in countering HIV-1 infection. To exert its anti-HIV-1 activity, A3G must be packaged into newly formed virions (Goila-Gaur and Strebel, 2008). During a second round of infection, A3G encapsidated in viral particles is delivered to the cytosol and blocks the replication of HIV-1. The antiviral competence of A3G is mainly ascribed to its cytidine deaminase activity, which introduce multiple G-to-A hypermutations into the HIV-1 genome, leading to malfunction or degradation (Chiu and Greene, 2008). In addition, certain cytidine deamination-independent mechanisms have recently been revealed (Bishop et al., 2008; Newman et al., 2005), suggesting comprehensive and complicated roles for A3G in antiviral responses. However, the role of A3G in host defense can be curbed by Vif, an HIV-1 regulatory protein essential for viral replication, by targeting A3G for polyubiquitination and proteasomal degradation, which prevents A3G's virion encapsidation and other underlying processes (Feng et al., 2013; Mariani et al., 2003; Marin et al., 2003; Yu et al., 2003). Cytosolic A3G may have little or no anti-HIV-1 activity, as suggested by previous researches in both T cell lines and transfected immortal HeLa and 293T cells, perhaps because endogenous and exogenous A3G can form large aggregates that prevent A3G's intrinsic deaminase activity (Chiu et al., 2005; Kreisberg et al., 2006).

Recently, we performed a computer-based prediction based on the PRISM (protein interactions by structural matching) algorithm, which uses structural and evolutionary similarities to find possible binary interactions within a target dataset based on similar known interfaces in a template dataset (Mashiach et al., 2010; Shatsky et al., 2004; Tuncbag et al., 2009, 2011) to screen for potential interactions between HIV-1 proteins and cellular restriction factors. The results suggested that Vpr (PDB: 1x9v) could interact with A3G (2jyw), with a similar interface as the A and B chains of 2ast, a known protein–protein interaction-pair model. Previous research has suggested that Vpr and A3G might jointly participate in certain processes. For example, Schrofelbauer noted that Vpr could facilitate HIV-1 infection by degrading UNG2 and SMUG1, which remove the uracil residues imported by A3G-catalyzed deamination (Schrofelbauer et al., 2005). Another group revealed that A3G activates the DNA damage response pathway (Norman et al., 2011), although it is widely agreed that this pathway can be triggered by Vpr (Rosenstiel et al., 2009; Ward et al., 2009).

In the present study, we confirmed the interaction of Vpr and A3G using the co-immunoprecipitation (Co-IP) method and demonstrated that Vpr could dramatically reduce the virion encapsidation of A3G. Vpr could induce the degradation of A3G through a VprBP binding and the proteasomal pathway. We also determined that the activity of Vpr in reducing A3G encapsidation, as described here, was correlated with Vpr's competence in inducing the degradation of A3G.

2. Materials and methods

2.1. PRISM algorithm and computer-based analysis

Compared with well-accepted templates, the potential interactions and interfaces between HIV-1 proteins such as Vif, Vpu, Vpr, and Capsid and host antiviral defenders such as A3G, Tetherin, SAMHD1, and the TRIM family proteins (128 target proteins) were screened using the PRISM algorithm. A representative 1036-template dataset of structurally non-redundant interfaces was generated using the PRISM protocol, and the biological interactions were outputted according to NOXclass. Four external programs, NACCESS, FASTA, MultiProt, and FiberDock, were incorporated into the PRISM protocol. In particular, FASTA was used to remove homologous chains; NACCESS was used to extract target protein surface regions; and MultiProt, which searches for spatial residue similarity, rather than sequential similarity, was used to evaluate the similarity between the individual target monomer surface regions and each side of a known template interface. The target protein surfaces that were similar to each part of the template interface were then transformed onto the template, forming a complex structure, and the solution was assessed. Ultimately, energies were calculated, and the predicted protein complexes were ranked using FiberDock, which can be used to resolve steric clashes, especially between side chains, and which ranks the putative complexes by global energy. The combination of geometric complementarity with docking procedures made the prediction results more accurate. All of the energy optimized complex structures of predicted interacting pairs were outputted by the PyMOL software.

2.2. Cells and plasmids

293T cells were cultured in Dulbecco's modified Eagle's medium (DMEM) (Gibco) supplemented with 1% glutamine and 10% fetal bovine serum (Gibco). The T lymphocyte cell lines MT4 and H9 were maintained in RPMI 1640 medium (Gibco) with additions as above. All cell cultures were grown at 37 °C with 5% CO_2.

Carboxyl-terminal HA- and Myc-tagged human A3G-expressing vectors were amplified from the total cDNA of H9 cells and then cloned into the pcDNA3.1 (+) backbone (Invitrogen). The HIV-1 proviral indicator constructs pNL4-3.Luc.F−R+ (pF−R+) (F and R represent *vif* and *vpr*, respectively) generated by inserting an NaeI linker at the PfiMI site of wild-type pNL4-3, pNL4-3.Luc.F+R− (pF+R−) (Adachi et al., 1986; Tokunaga et al., 2001; Zheng et al., 2004); the pseudo-viral membrane protein vector pVpack-VSV-G (Koyama et al., 2013); and the Flag-tagged Vif-expressing vector (NL4-3-derived) (Iwabu et al., 2010) have been previously described. The *vif* and *vpr* double-deletion (Δ*vif* Δ*vpr*) HIV-1 pseudo-viral plasmid pNL4-3.Luc.F−R− (pF−R−) was constructed through a recombination method based on pF−R+ and pF+R−. Flag-tagged wild-type Vpr was a kind gift from Yukihito Ishizaka. Flag-tagged VprQ65R was mutated using KOD-dependent PCR (TOYOBO) based on wild-type Flag-Vpr. A human VprBP expression vector with an amino-terminal HA tag was amplified from the total cDNA of 293T cells and cloned into pcDNA3.1 (+). The EGFP expressing vector pEGFP-N2 was purchased from Clontech.

2.3. Transfection

To reach >80% confluency prior to transient transfection, 293T cells were seeded in plates for overnight culture. Plasmids in the indicated combinations were transfected into cells using the FuGENE HD Transfection Reagent (Promega) according to the manufacturer's instructions. For certain experiments, proteasome inhibitor MG132 (Sigma) with the final concentration of 12.5 μM and the equivalent volume of control reagent DMSO (Sigma) were added to the cell cultures after 24 h of transfection for another 16 h of incubation, followed by cell harvesting and specific assays.

For RNAi-based gene knock-down, siRNA for human VprBP, with the sequence of 5′-GGCAGCTGAAGCTCTATAA-3′, and control RNA were synthesized (RIBOBIO) and then transfected into 293T cells at a concentration of 50 nM in combination with other indicated plasmids using Lipofectamine 2000 (Invitrogen) following the manufacturer's instructions. The culture medium was changed at 6 h and 48 h post-transfection, and the cells were harvested for immunoblot analysis after a total incubation of 72 h.

2.4. Virus production and infection

Virus stocks encoding the luciferase reporter gene were produced by transfecting HIV-1 proviral constructs, pVpack-VSV-G and other relevant plasmids into 293T cells using FuGENE HD. One day later, the cell medium was refreshed, followed by incubation for another 24 h. The supernatants were then harvested and centrifuged to remove debris. The supernatants were filtered at 0.45 μm and subjected to quantification using an HIV-1 p24 ELISA (Advanced BioScience Laboratories).

Cell lines plated one day earlier were infected with normalized virions at specific concentrations. Next, 24 or 48 h later, the cells were precipitated, washed twice with 1× PBS (Gibco), and then used in assays such as immunoblotting, luciferase reporter assays and qPCR.

2.5. Luciferase reporter assay

Cells infected with HIV-1 reporter pseudo-viruses were collected, washed twice with 1× PBS and then assayed using the Luciferase Assay System (Promega) following the manufacturer's instructions. The luciferase activity data were calibrated by total protein quantification of the cell samples using the BCA method (Beyotime).

2.6. Immunoblot analysis

Proteins derived from cells and virions were obtained from different experiments. For cellular proteins, a cell precipitate was lysed on ice with a basic cell lysis buffer (with 100 μM PMSF) (Beyotime), and protein samples were prepared as previously described (Chen et al., 2012). For virion proteins, virus (equivalent to 300 ng of p24) precipitated using PEG-*it* virus precipitation solution (5×) (SBI) was lysed and boiled in a defined amount of Laemmli sample buffer (containing 1/19 volume of β-ME) (Bio-Rad). The prepared protein samples were used to perform immunoblot analysis as described previously (Chen et al., 2012). The antibodies used were anti-HA MAb and anti-Flag MAb, purchased from Sigma; anti-HIV-1 p24 MAb, anti-Myc MAb, anti-A3G MAb and anti-VprBP MAb, from Santa Cruz Biotechnology; anti-β-actin MAb, from ZSGB-BIO; mouse control IgG, from Boster; anti-GAPDH MAb and anti-EGFP MAb, from Beyotime; HRP-linked anti-mouse/rabbit secondary antibody, from Cell Signaling Technology; and anti-Vpr MAb, which was a kind gift from Yukihito Ishizaka.

2.7. Co-immunoprecipitation (Co-IP) analysis

Transfected 293T cells cultured in 60-mm dishes were collected, washed twice with 1× PBS, gently resuspended in 450 μl of IP buffer (50 mM Tris, 1 mM EGTA, 1 mM EDTA, 1% Triton X-100, 150 mM NaCl, 2 mM DTT, 100 μM PMSF, and 1 μg/ml proteinase inhibitors purchased from Roche, pH 7.4) and placed on a vibrating mixer at 4 °C for 20 min. The cell lysate was then centrifuged, and the supernatant was separated into two aliquots. One aliquot of 400 μl was mixed with prewashed (with IP buffer, followed by centrifugation) protein G agarose (Millipore), together with 1 μg of the indicated antibodies (control mouse IgG and anti-Myc MAb), and placed on a rotational tumbler for incubation overnight at 4 °C. The agarose was washed with IP buffer and boiled in 50 μl of Laemmli sample buffer (containing 1/19 volume of β-ME), serving as the IP sample. Another aliquot of 40 μl of supernatant was boiled in sample loading buffer (5×) (Beyotime), serving as the input sample. All of the samples were analyzed by immunoblotting.

2.8. Real-time quantitative PCR assay

Infected H9 cells were harvested after 48 h of incubation and washed twice with 1× PBS, after which total RNA was extracted with TRIzol reagent (Invitrogen). The RNA samples were immediately reverse transcribed by M-MLV RT (Promega) to produce cDNA, which was then detected by real-time qPCR with the primers 5′-TCAGAGGACGGCATGAGACTTAC-3′ (sense) and 5′-AGCAGGACCCAGGTGTCATTG-3′ (anti-sense) (Chen et al., 2006) and using SYBR Green SuperMix (Invitrogen) according to the manufacturer's instructions.

2.9. Statistical analysis

The data from the luciferase reporter assay and qPCR assay are presented as the mean ± SD of three independent experiments, and all analyses were performed using Student's *t*-test. $P < 0.01$ (*) was considered statistically significant.

3. Results

3.1. HIV-1 Vpr forms a binary complex with A3G

To reveal the cryptic interactions between the proteins of HIV-1 and host cells, we first used PRISM to screen for potential physical interactions and their interfaces in the virus-host interactive network. The target dataset considered here included HIV-1 proteins and HIV restriction factors with known structures stored in the PDB database. The results indicated that not only Vif but also Vpr interacted with A3G (Fig. 1A) and that the interface between them was similar to that of 2astAB, i.e., the interface of the 2ast (the crystal structure of Skp1-Skp2-Cks1 in complex with a p27 peptide) A and B chains, consisting of S-phase kinase-associated protein 1A and S-phase kinase-associated protein 2 separately (Fig. 1B and C). These bioinformatics results suggest that Vpr directly interacts with A3G.

Previous research demonstrated that Vpr interacts with many cell proteins to form functional complexes (Klockow et al., 2013; Maudet et al., 2013; Okumura et al., 2008; Schrofelbauer et al., 2005; Wang et al., 2013; Zhao et al., 2011). Based on our prediction results, we tested the interaction of Vpr and A3G by a Co-IP approach. Flag-tagged Vpr and Myc-tagged A3G were transfected, either separately or together, into 293T cells. Forty hours post-transfection, all of the samples were lysed, and Co-IP was performed. We found that Vpr could co-precipitate with A3G (Fig. 1D). This result confirms our computational prediction that Vpr interacts with A3G.

3.2. HIV-1 Vpr reduces the virion encapsidation of A3G

The prominent anti-HIV-1 activity of A3G requires A3G encapsidation into progeny viral particles (Goila-Gaur and Strebel, 2008). Because the interaction of Vpr and A3G had been verified, we next investigated whether the intracellular operation of A3G, particularly its virion encapsidation and antiviral effect, could be influenced by Vpr. We first sought to establish the A3G encapsidation system before performing our studies and to test the implication of this encapsidation for anti-HIV-1 activity. Δ*vif* Δ*vpr* HIV-1 virions were produced by transfecting 293T cells coupled with an increasing amount of HA-tagged A3G-expressing vector. The virions were calibrated with p24 and concentrated using PEG-*it*. The protein levels in the virions and virion-producing cells were detected by immunoblotting. The results in Fig. 2A show that A3G-HA was successfully encapsidated into new virions according to the expected increasing amounts. Additionally, 293T cells were infected with the virions, and after 24 h of incubation, the target cells were lysed and subjected to a luciferase reporter assay. As the

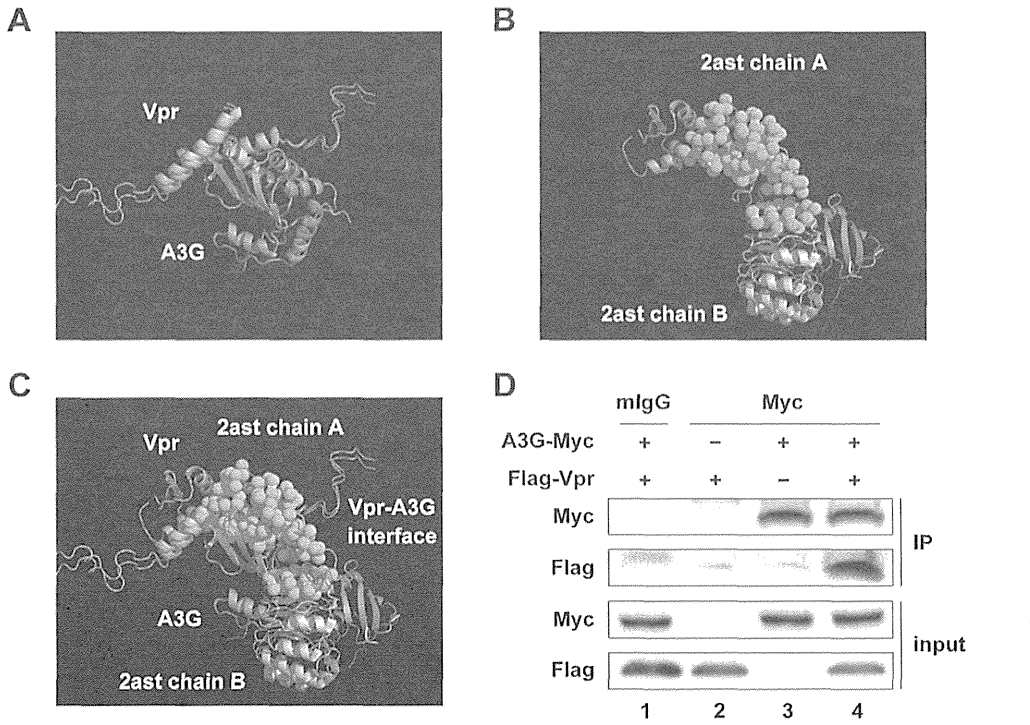

Fig. 1. HIV-1 Vpr interacts with A3G. (A) The schematic of the interaction between Vpr and A3G predicted by the PRISM algorithm using the A and B chains of 2ast as a template. (B) The interaction of the A and B chains of 2ast, used as a template (the green spots represent the interface). (C) The interface of Vpr and A3G is similar to that of the A and B chains of 2ast. (D) The predicted interaction of Vpr and A3G was confirmed by the Co-IP method. For this purpose, 293T cells were transfected with A3G-Myc (4 μg in lanes 1 and 4 co-transfected with Flag-Vpr and 2 μg in lane 3) and Flag-Vpr (2 μg) in different combinations, as depicted. Cells were treated with MG132 overnight before harvesting. Cell lysates were used for Co-IP with control mouse IgG (mIgG) (lane 1) and anti-Myc MAb (lanes 2–4). The IP samples and raw lysates (input) were detected by immunoblotting with the indicated antibodies. (For interpretation of the references to color in this figure legend, the reader is referred to the web version of this article.)

quantity of virion-associated A3G increased, HIV-1 infectivity was markedly and gradually inhibited (Fig. 2B).

Next, we tested the anti-HIV-1 effect of cytosolic A3G. One day after 293T cells were transfected with an increasing amount of A3G-HA, we used *Δvif Δvpr* HIV-1 virions containing no A3G to infect these cells for another 24 h. Cell lysates were then analyzed by luciferase reporter and immunoblot assays. Fig. 2C shows that despite the different but sufficient amounts of A3G synthesized in the cytosol of the target 293T cells, the infectivity of HIV-1 was unchanged. These results show that the anti-HIV-1 activity of A3G is dictated by the status of its virion association.

The encapsidation of A3G into new virions is so important that theoretically, curbing the efficiency of this process is one of the most impactful tactics to neutralize this HIV-1 restriction factor. Using the experimental system established above, we examined the modulation of A3G encapsidation by Vpr. The expression vectors A3G-HA and Flag-Vpr, together with pF–R– and pVpack-VSV-G, were transfected into 293T cells to produce A3G-associated *Δvif Δvpr* HIV-1 virions containing or not containing the Vpr protein. We precipitated and normalized these virions, followed by detection of the proteins in cells and virions by immunoblotting. The existence of Vpr strongly reduced the amount of A3G enclosed in HIV-1 virions compared with the amount in the group solely transfected with A3G-HA (Fig. 2D).

To clarify whether the reduction of A3G encapsidation by Vpr affects virus infectivity, we infected the T lymphocyte cell line MT4 with harvested virions (Fig. 2D). After an incubation of 24 h, the cells were subjected to a luciferase reporter assay. The results show that the infectivity of virions containing a smaller quantity of A3G due to Vpr activity (Fig. 2E, lane 4) was stronger than in the group solely transfected with A3G (Fig. 2E, lane 3); that is, Vpr significantly increased the infectivity of HIV-1 inhibited by virion-encapsidated A3G. In conclusion, Vpr strikingly decreases the virion encapsidation of A3G, affecting A3G's anti-HIV-1 activity.

Since Vpr shares the anti-A3G activity with Vif, it could be interesting and necessary to compare the neutralizing efficiency of these two HIV-1 accessory proteins. For this purpose, *Δvif Δvpr* HIV-1 virions were produced from 293T cells by co-transfecting with pF–R–, pVpack-VSV-G, A3G-HA and Flag-Vpr or Flag-Vif. Normalized virions and virion-producing cells were lysed for immunoblotting (Fig. 2F). Meanwhile, the corresponding virions were separated into two groups, Vpr-associated group (lanes 1, 2, 4, 5 of Fig. 2F) and Vif-associated group (lanes 1, 3, 4, 6 of Fig. 2F) for the test of viral infectivity (Fig. 2G and H). These data show that, Vif almost entirely inhibited the encapsidation of A3G, resulting in an extremely significant recovery of HIV-1 infection blocked by A3G, while in comparison, such effect of Vpr was moderate.

3.3. *Vpr decreases the protein level of A3G*

The results in Fig. 2D and F suggested that Vpr might reduce the protein level of A3G. To clarify the interplay between Vpr and A3G, we co-transfected A3G-HA and an increasing amount of Flag-Vpr into 293T cells and detected the levels of the indicated proteins (Fig. 3A). The transfected EGFP was used as the internal control and the ratio of immunoblot signals for A3G and EGFP was calculated (Fig. 3B). These results show that Vpr induced a significant decrease in exogenously transfected A3G in a dose-dependent manner.

We also investigated the effect of Vpr on endogenous A3G. Two types of HIV-1 pseudo-viruses, NL4-3.Luc.F–R– (F–R–) and

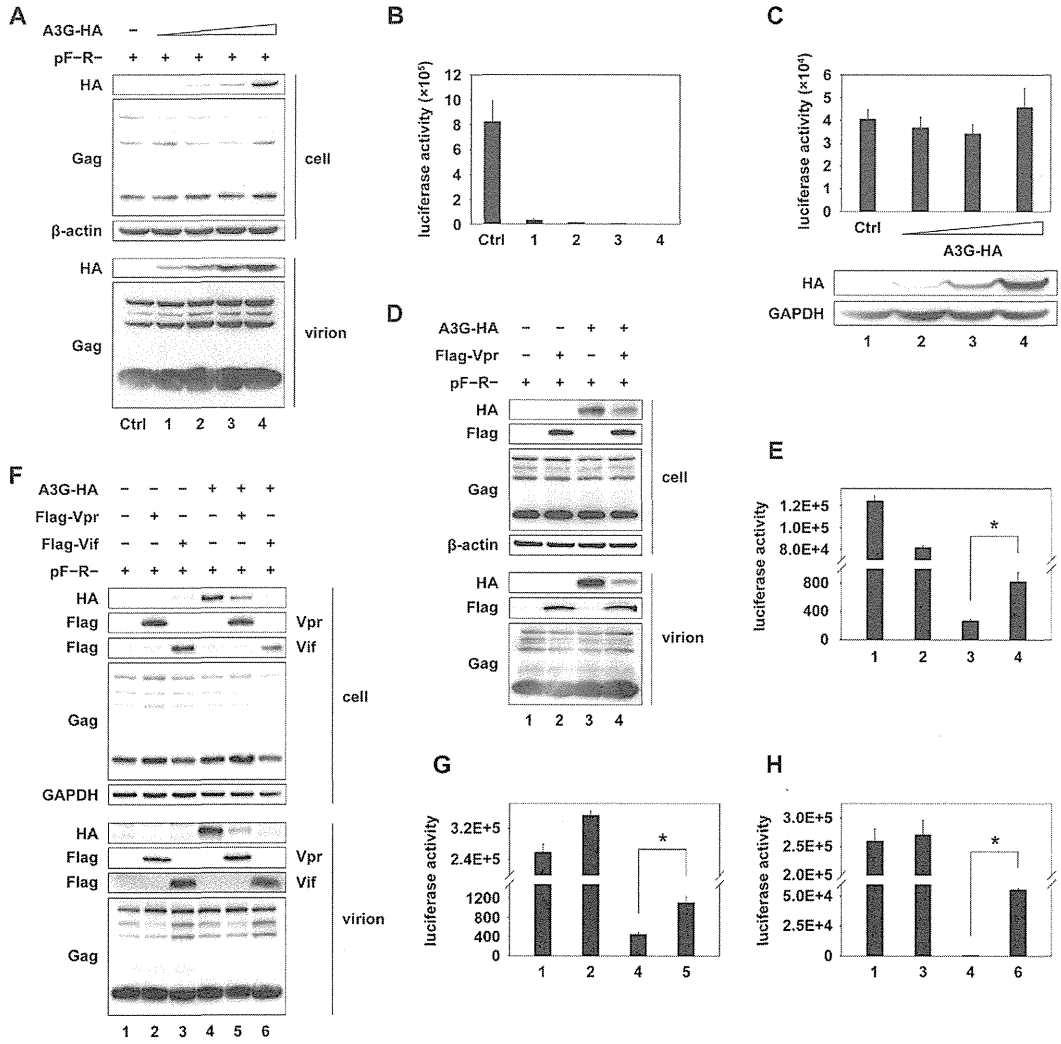

Fig. 2. The virion encapsidation of A3G is reduced by Vpr. (A) A3G can be encapsidateed into HIV-1 pseudo-viral particles. Δ*vif* Δ*vpr* HIV-1 virions were produced from 100-mm dishes of 293T cells by co-transfection with pF−R−, pVpack-VSV-G and an increasing amount of A3G-HA (0 μg, 0.5 μg, 1 μg, 2 μg, and 5 μg). Equal quantities of normalized virions were precipitated by PEG-*it* and subjected, together with virion-producing cells, to immunoblotting with the indicated antibodies. Gag and β-actin were used as internal controls. (B) HIV-1 infectivity is inhibited by virion-associated A3G. Virions containing the A3G-HA packed in (A) were used to infect 293T cells at a concentration of 25 ng/ml. Twenty-four hours later, the cells were collected and used for a luciferase reporter assay. (C) Cytosolic A3G lacks the anti-HIV-1 effect. Twelve-well plates of 293T cells were transfected with an increasing amount of A3G-HA (0.1 μg, 0.2 μg, and 0.5 μg), followed by infection with 50 ng/ml A3G-free Δ*vif* Δ*vpr* pseudo-HIV-1 virions one day later. Luciferase activity was examined after another 24 h of culture, and the protein level of A3G and GAPDH was detected by immunoblotting. (D) Vpr reduces the encapsidation of A3G into HIV-1 pseudo-viral particles. Δ*vif* Δ*vpr* HIV-1 virions were produced from 100-mm dishes of 293T cells by co-transfection with pF−R−, pVpack-VSV-G, A3G-HA (2.5 μg) and Flag-Vpr (2.5 μg) in the indicated combinations. Harvested virions normalized to p24 were concentrated, and the proteins in the virions and virion-producing cells were analyzed by immunoblotting with the indicated antibodies. (E) The inhibition of HIV-1 infection by A3G is partially recovered by Vpr. The normalized virions collected in (D) were used to infect MT4 cells at a concentration of 25 ng/ml. After 24 h of incubation, the cells were collected and subjected to a luciferase reporter assay. (F, G and H) The Vif's effect on curbing the anti-HIV-1 activity of A3G is stronger than that of Vpr. Δ*vif* Δ*vpr* HIV-1 virions were produced by co-transfection with pF−R−, pVpack-VSV-G, A3G-HA (2.5 μg), Flag-Vpr (2.5 μg) and Flag-Vif (2.5 μg) in the indicated combinations. Proteins were analyzed by immunoblotting as (D). Meanwhile, the corresponding virions of Vpr-associated group (lanes 1, 2, 4, 5) and Vif-associated group (lanes 1, 3, 4, 6) were used to infect MT4 cells, followed by luciferase reporter assay as (E) (*$P < 0.01$, Student's *t*-test).

NL4-3.Luc.F−R+ (F−R+), were used to infect H9 cells, a category of T lymphocyte that endogenously produces A3G. Forty-eight hours after infection, the cells were collected and divided into two aliquots to determine the A3G protein and mRNA levels. Similar to the results for the ectopic expression of A3G, the endogenous A3G level was decreased by Vpr (Fig. 3C). A qPCR assay indicated that a reduction in A3G levels does not occur during transcription because the quantity of A3G mRNA was not affected by Vpr (Fig. 3D). These data are the first to demonstrate that Vpr can downregulate the protein level of A3G.

3.4. *Vpr induces the degradation of A3G through VprBP binding and a proteasomal pathway*

Next, we demonstrated the mechanism of the downregulation of A3G by Vpr. Considering that the previously reported effect of Vpr on decreasing the protein level of substrates was VprBP-triggered proteasomal degradation, we investigated the role of VprBP in the Vpr-mediated downregulation of A3G. We used Flag-tagged VprQ65R, a mutant of Vpr deficient in binding VprBP (Le Rouzic et al., 2007), Flag-Vpr, and A3G-HA to transfect 293T cells

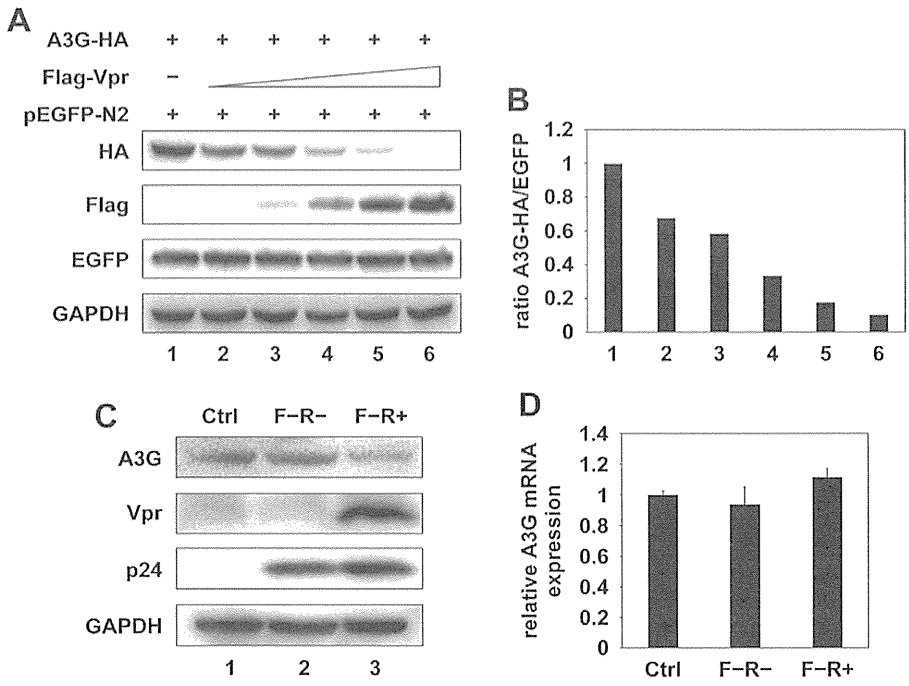

Fig. 3. Vpr downregulates the protein level of A3G. (A) Vpr reduces the protein level of A3G in a dose-dependent manner. A3G-HA (0.8 μg), pEGFP-N2 (0.08 μg) and an increasing amount of Flag-Vpr (0 μg, 0.1 μg, 0.2 μg, 0.4 μg, 0.8 μg, and 1.2 μg) were co-transfected into 6-well plates of 293T cells, followed by 24 h of incubation. The protein levels of A3G and Vpr were detected by immunoblotting with the indicated antibodies. (B) The ratio of immunoblot signals for A3G-HA and EGFP was calculated from (A). (C) Vpr downregulates the protein level of endogenous A3G (D) but does not affect transcription. H9 cells were infected with F–R– or F–R+ at a concentration of 50 ng/ml. The control group was treated with an equivalent volume of DMEM. Forty-eight hours post-infection, one portion of the cells was lysed for immunoblot analysis with the indicated antibodies, whereas the other, unlysed portion was subjected to total RNA extraction, followed by reverse transcription and qPCR testing for A3G mRNA.

in the indicated combinations. Flag-tagged Vif was used as the positive control. The cells were cultured for 40 h and lysed for immunoblot analysis. As shown in Fig. 4A, even though the expression of VprQ65R was stronger than that of wild-type Vpr, despite transfection of the same amount of DNA, this mutant failed to decrease the expression of A3G. This result suggests that the interaction of Vpr and VprBP is necessary for Vpr to down-modulate A3G.

To more clearly understand the relevance of VprBP, we performed two series of experiments with opposite strategies. First, we co-transfected A3G-HA, HA-tagged VprBP, Flag-Vpr, Flag-VprQ65R and Flag-Vif into 293T cells in the indicated combinations, followed by immunoblot analysis to observe the consequence of overexpressing VprBP. Fig. 4B shows that when there was a large quantity of VprBP, the degree of downregulation of A3G increased remarkably, regardless of whether A3G encountered Vpr or VprQ65R (not Vif), and transfected Vpr and Vif (not VprQ65R) could enhance the degree of VprBP-mediated downregulation of A3G (Fig. 4C). Fig. 4D shows that solely overexpression of VprBP (without any viral proteins) could reduce the protein level of A3G significantly, which was consistent with the phenomenon depicted from Fig. 4B and C. Second, an experiment using siRNA for VprBP found that when VprBP was silenced, the downregulation of A3G maintained by Vpr was nearly completely abrogated (Fig. 4E), while when silencing VprBP, the degree of Vif-induced degradation of A3G was not disturbed severely (Fig. 4F). These results strongly suggest that VprBP, being able to decrease the protein level of A3G without any viral proteins, is absolutely necessary in the Vpr-mediated downregulation of A3G.

In order to further confirm the significance of VprBP in Vpr-induced downregulation of A3G, we tested the interaction of VprQ65R and A3G using the Co-IP method. 293T cells were co-transfected with Flag-Vpr, Flag-VprQ65R and Myc-A3G in the indicated combinations, and forty hours post-transfection, all of the samples were lysed for Co-IP analysis. We found that VprQ65R mutant could interact with A3G (Fig. 4G). This result excludes the possibility that the lack of VprQ65R in downregulating A3G is attributed to a loss of binding to A3G.

Due to the essential role of VprBP in assisting Vpr in triggering the degradation of putative host proteins (DeHart and Planelles, 2008), we studied whether the Vpr-regulated downregulation of A3G occurs via proteasomal degradation. MG132 with the final concentration of 12.5 μM were applied after co-transfecting 293T cells with A3G-HA, Flag-Vpr, Flag-VprQ65R, Flag-Vif and pEGFP-N2 in the indicated combinations. The immunoblot results and the calculation for their signals show that MG132 recovered the Vpr-mediated inhibition of A3G expression compared with control treatment (equivalent volumes of DMSO) (Fig. 4H and I). Thus, we are confident that the downregulation of A3G expression by Vpr is due to proteasome-dependent degradation. Altogether, our results confirm that Vpr induces the degradation of A3G through VprBP binding and participation of the proteasome.

3.5. A3G degradation by Vpr leads to a reduction in A3G encapsidation

What is the fundamental mechanism granting Vpr the ability to reduce A3G encapsidation? To further explore whether Vpr-mediated A3G degradation leads to decreased A3G encapsidation, A3G-associated HIV-1 virions were produced by transfecting pF–R–, pVpack-VSV-G, A3G-HA, and Flag-Vpr or Flag-VprQ65R into 293T cells, followed by virion normalization, precipitation and immunoblot analysis. The level of A3G in VprQ65R-associated virions (Fig. 5A, lane 5) was higher than that in wild-type Vpr-associated virions (Fig. 5A, lane 4) and similar to that in Vpr-absent virions (Fig. 5A, lane 3). These results suggest that VprQ65R does

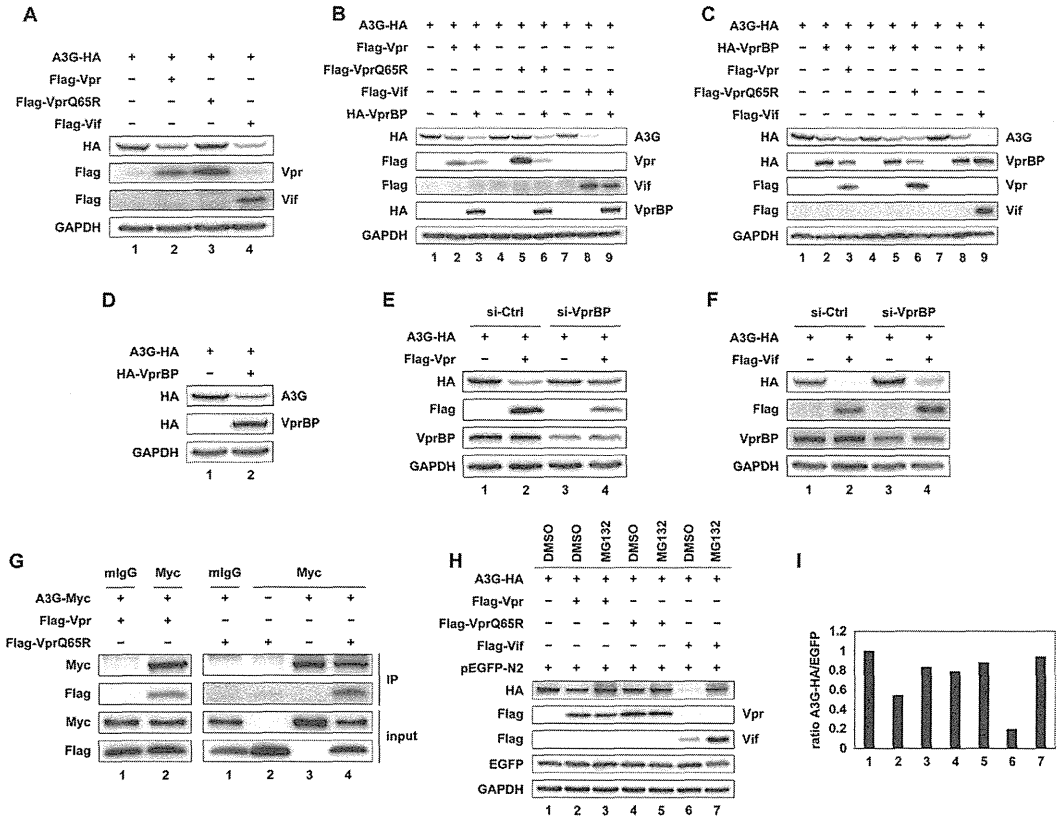

Fig. 4. Vpr induces the degradation of A3G through a VprBP-mediated proteasomal pathway. (A) VprQ65R fails to decrease the expression of A3G. Six-well plates of 293T cells were co-transfected with the indicated expression vectors (1 μg). Forty hours later, the cells were lysed for immunoblot analysis with the indicated antibodies. (B) Overexpression of VprBP aggravates the Vpr-mediated downregulation of A3G. Six-well plates of 293T cells were co-transfected with the indicated expression vectors (0.8 μg). After 40 h of culture, the cells were analyzed by immunoblotting with the indicated antibodies. (C) VprQ65R lacks the effect of Vpr and Vif on promoting the VprBP-mediated downregulation of A3G. Expression vectors of 0.8 μg were co-transfected in the indicated combinations, followed by immunoblotting after 40 h of culture. (D) VprBP is able to downregulate the expression of A3G. Six-well plates of 293T cells were co-transfected with A3G-HA (1 μg) and HA-VprBP (1.2 μg). Forty hours later, the cells were lysed and analyzed by immunoblotting. (E) Silencing of endogenous VprBP diminishes Vpr-induced A3G downregulation. In total, 50 nM VprBP siRNA and control siRNA were transfected into 6-well plates of 293T cells, with or without A3G-HA (1 μg) and Flag-Vpr (1 μg). After 72 h of culture, the cells were lysed and used for immunoblot analysis with the indicated antibodies. (F) The effect of VprBP silence on Vif-induced A3G downregulation was used as a control. (G) VprQ65R mutant interacts with A3G. 293T cells were transfected with A3G-Myc (4 μg), Flag-Vpr (2 μg) and Flag-VprQ65R (2 μg) in depicted combinations, Cells were treated with MG132 overnight before harvesting, followed by Co-IP and immunoblot analysis. (H) Vpr triggers A3G degradation through the proteasomal pathway. Six-well plates of 293T cells were co-transfected with A3G-HA (1 μg), Flag-Vpr (1 μg), Flag-VprQ65R (1 μg), Flag-Vif (1 μg) and pEGFP-N2 (0.1 μg) in the indicated combinations. After 24 h, the cells were treated overnight with 12.5 μM MG132 or an equivalent volume of DMSO, followed by protein extraction and immunoblot analysis with the indicated antibodies. (I) The ratio of immunoblot signals for A3G-HA and EGFP was calculated from (H).

not reduce A3G encapsidation. Consistent results were obtained from the infection experiment depicted in Fig. 5C, showing that the replicative capability of HIV-1 pseudo-virions was inversely proportional to their embedded quantity of A3G. These observations demonstrate that the ability of Vpr to recruit a VprBP-dependent E3 ubiquitin ligase complex and to induce the degradation of A3G is the critical reason for the Vpr-mediated reduction of A3G encapsidation.

4. Discussion

Ongoing theoretical research on the mutual effects of HIV-1 accessory proteins and host antiviral agents has been an extremely important field ever since the first identification of HIV-1 particles. At the start of our research, we used a computational approach called PRISM to seek bioinformatics clues to undiscovered interactions between HIV-1 and host proteins. Computational analysis, combined with Co-IP results, informed us that Vpr could interact with A3G to form a binary aggregate. This conclusion was surprising because in contrast to Vif, no one has ever considered the possibility of Vpr relating so closely with A3G. Our subsequent experiments demonstrated that (i) the virion encapsidation of A3G, the crucial step for countering the HIV-1 life cycle, can be efficiently reduced by Vpr, (ii) Vpr can induce the degradation of A3G through VprBP binding and the proteasomal pathway, and (iii) the activity of Vpr in curbing A3G virion encapsidation can be ascribed to this proteasome-dependent degradation.

A3G, a type of enzyme associated with "RNA editing," has been viewed as a fundamental and essential protector that maintains the stability of cells by defending against the invasion of exogenous viruses and the overactivation of endogenous retro-elements (Esnault et al., 2005; Kinomoto et al., 2007; Muckenfuss et al., 2006). The antiviral ability of A3G is so effective that in one study, only 7 ± 4 A3G molecules were incorporated into Δ*vif* virions derived from PBMCs, yet such a small amount exerted remarkable anti-HIV-1 activity (Xu et al., 2007). In fact, some of our infection experiments (Fig. 2E, G, H and Fig. 5C) indicated that the recovery of HIV-1 infectivity boosted by Vpr and Vif did not achieve the level in the control lacking A3G. Although Vpr and Vif could significantly reduce the expression of A3G, this reduction was not exhaustive under the condition of exogenous transfection, and the remaining A3G was sufficient for virion encapsidation to keep the replication of HIV-1

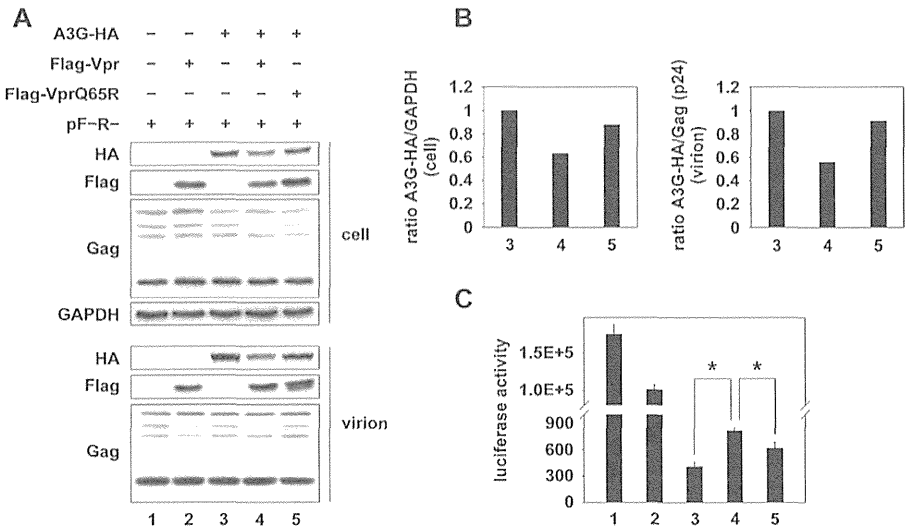

Fig. 5. The reduction in A3G encapsidation by Vpr is correlated with Vpr-mediated A3G degradation. (A) VprQ65R has impaired competence in reducing the virion encapsidation of A3G. Δ*vif* Δ*vpr* HIV-1 virions were produced from 100-mm dishes of 293T cells by co-transfection with pF−R−, pVpack-VSV-G, A3G-HA (2.5 μg), Flag-Vpr (2.5 μg) or VprQ65R (2.5 μg). The virions were then normalized and precipitated, and the proteins in the virions and virion-producing cells were analyzed by immunoblotting with the indicated antibodies. (B) The ratio of immunoblot signals for A3G-HA and GAPDH (cell) or p24 (virion) was calculated from (A). (C) The infectivity of HIV-1 pseudo-virions is inversely proportional to their amount of encapsidated A3G. Normalized virions harvested from (A) were used to infect MT4 cells. After 24 h, the cells were collected and used for luciferase reporter assays (*$P < 0.01$, Student's *t*-test).

low. So far, a lot of efforts have been put into the study of Vif-A3G interaction which is becoming more and more explicit. However, few studies have focused on the relationship of A3G and other HIV-1 accessory proteins, such as Vpr, despite the non-negligible evidence mentioned earlier.

One of the earliest discovered host factors relevant to Vpr is UNG2. The role played by UNG2 in the HIV-1 life cycle is still controversial, and conflicting data have been reported (Chen et al., 2004; Guenzel et al., 2012; Jones et al., 2010; Priet et al., 2005; Schrofelbauer et al., 2005; Weil et al., 2013; Yan et al., 2011; Yang et al., 2007), whereas the fact that UNG2 can be degraded by Vpr through the proteasomal pathway is widely recognized. An early viewpoint worthy of remark was that, the anti-HIV-1 effect of A3G could be partially recovered by Vpr through degrading UNG2, who can work together with A3G to block HIV-1 replication (Schrofelbauer et al., 2005). Subsequent studies, however, questioned this conclusion by arguing that when deficient in UNG2, the replication of HIV-1 cannot be disturbed, regardless of the presence of A3G (Kaiser and Emerman, 2006; Langlois and Neuberger, 2008). Since that time, much work has been devoted to unveiling the puzzling function of UNG2, yet most studies have not paid due attention to the potential effect directly exerted by Vpr on A3G.

The complicated interplay between HIV-1 accessory proteins and host agents always usurps the cellular ubiquitination and the proteasome-mediated degradation system (Biard-Piechaczyk et al., 2012). Specifically, Vif recruits Cul5 ubiquitin ligase to downregulate A3G (Iwatani et al., 2009; Yu et al., 2003), Vpr degrades UNG2 via the Cul4A-DDB1-VprBP ubiquitin ligase complex (Ahn et al., 2010; Schrofelbauer et al., 2005, 2007), and Vpu poly-ubiquitinates CD4 and subjects it to proteasomal degradation (Binette et al., 2007; Magadan et al., 2010). These conclusions have been gradually acknowledged over the past decades. However, nearly all of these results were obtained during investigating Vif-A3G, Vpr-UNG2 and Vpu-CD4 pairs independently, and few research teams have concentrated on the intricate yet likely crosstalk between them. Here, we showed that besides Vif, Vpr could also mediate the degradation of A3G. Thus such crosstalk has been verified for the first time by showing that A3G could be degraded by ether a Vpr-mediated, VprBP-dependent E3 ubiquitin ligase complex or a Vif-mediated Cul5-SCF complex. It is necessary to mention that as implied in Fig. 4B, C and D, VprBP alone was sufficient to induce the degradation of A3G, whereas Vpr acted to enhance the extent of, rather than to enable, this degradation. Such interesting and slightly perplexing results have been mentioned in some recent reports (Nakagawa et al., 2013; Wen et al., 2012), and obtaining more accurate details will require systematic and intensive follow-up studies.

In Fig. 5C, we noticed that the infectivity of virions associated with VprQ65R (lane 5) was stronger than in the absence of any type of Vpr (lane 3). In fact, Fig. 5A shows that the amount of virion-associated A3G co-existing with VprQ65R (lane 5) was less than in the A3G-alone group (lane 3), consistent with the infection results in Fig. 5C. The difference in the amount of A3G enclosed in virions was ascribed to dissimilar expression of A3G in virion-producing cells co-transfected with empty vector or VprQ65R (Fig. 5B, left panel). Even if VprBP is deficient in VprBP binding activity, the degradation-inducing ability of this mutant seemed not to be completely lost, and some previous reports showed that the VprQ65R mutant could slightly downregulate the substrates of Vpr (Klockow et al., 2013; Maudet et al., 2013).

In summary, we demonstrated that in addition to Vif, Vpr could also prevent A3G from encapsidation in newly budded HIV-1 virions by subjecting this host restriction factor to the VprBP-mediated proteasomal degradation pathway. The crosstalk between the Vif-Cul5 and the Vpr-VprBP-E3 ubiquitin systems suggested by our data reveals the subtlety of virus-host interplay, which remains far from understood. Future investigations and more concentrated efforts should be dedicated to systematic research on HIV-1 accessory proteins and antiviral agents, rather than isolated investment, and the accumulated conclusions will inevitably expose more details about HIV-1 pathogenesis.

Acknowledgments

We appreciate Yukihito Ishizaka (National Center for Global Health and Medicine, Japan) for generously providing plasmids and other reagents. This work was supported by the grants of

the Key National Science and Technology Program in the 12th Five-Year Period (Grant 2012ZX10001-006), the Key Laboratory on Emerging Infectious Disease and Biosafety in Wuhan and the International Science & Technology Cooperation Program of China (2011DFA31030) and Deutsche Forschungsgemeinschaft (SFB/Transregio TRR60).

References

Adachi, A., Gendelman, H.E., Koenig, S., Folks, T., Willey, R., Rabson, A., Martin, M.A., 1986. Production of acquired immunodeficiency syndrome-associated retrovirus in human and nonhuman cells transfected with an infectious molecular clone. J. Virol. 59 (2), 284–291.

Ahn, J., Vu, T., Novince, Z., Guerrero-Santoro, J., Rapic-Otrin, V., Gronenborn, A.M., 2010. HIV-1 Vpr loads uracil DNA glycosylase-2 onto DCAF1, a substrate recognition subunit of a cullin 4A-ring E3 ubiquitin ligase for proteasome-dependent degradation. J. Biol. Chem. 285 (48), 37333–37341.

Biard-Piechaczyk, M., Borel, S., Espert, L., de Bettignies, G., Coux, O., 2012. HIV-1, ubiquitin and ubiquitin-like proteins: the dialectic interactions of a virus with a sophisticated network of post-translational modifications. Biol. Cell 104 (3), 165–187.

Binette, J., Dube, M., Mercier, J., Halawani, D., Latterich, M., Cohen, E.A., 2007. Requirements for the selective degradation of CD4 receptor molecules by the human immunodeficiency virus type 1 Vpu protein in the endoplasmic reticulum. Retrovirology 4, 75.

Bishop, K.N., Verma, M., Kim, E.Y., Wolinsky, S.M., Malim, M.H., 2008. APOBEC3G inhibits elongation of HIV-1 reverse transcripts. PLoS Pathog. 4 (12), e1000231.

Chen, C., Qiu, H., Gong, J., Liu, Q., Xiao, H., Chen, X.W., Sun, B.L., Yang, R.G., 2012. (−)-Epigallocatechin-3-gallate inhibits the replication cycle of hepatitis C virus. Arch. Virol. 157 (7), 1301–1312.

Chen, K., Huang, J., Zhang, C., Huang, S., Nunnari, G., Wang, F.X., Tong, X., Gao, L., Nikisher, K., Zhang, H., 2006. Alpha interferon potently enhances the anti-human immunodeficiency virus type 1 activity of APOBEC3G in resting primary CD4T cells. J. Virol. 80 (15), 7645–7657.

Chen, R.X., Le Rouzic, E., Kearney, J.A., Mansky, L.M., Benichou, S., 2004. Vpr-mediated incorporation of UNG2 into HIV-1 particles is required to modulate the virus mutation rate and for replication in macrophages. J. Biol. Chem. 279 (27), 28419–28425.

Chiu, Y.L., Greene, W.C., 2008. The APOBEC3 cytidine deaminases: an innate defensive network opposing exogenous retroviruses and endogenous retroelements. Annu. Rev. Immunol. 26, 317–353.

Chiu, Y.L., Soros, V.B., Kreisberg, J.F., Stopak, K., Yonemoto, W., Greene, W.C., 2005. Cellular APOBEC3G restricts HIV-1 infection in resting CD4(+) T cells (Retracted Article. See vol. 466, pg 276, 2010). Nature 435 (7038), 108–114.

DeHart, J.L., Planelles, V., 2008. Human immunodeficiency virus type 1 vpr links proteasomal degradation and checkpoint activation. J. Virol. 82 (3), 1066–1072.

Esnault, C., Heidmann, O., Delebecque, F., Dewannieux, M., Ribet, D., Hance, A.J., Heidmann, T., Schwartz, O., 2005. APOBEC3G cytidine deaminase inhibits retrotransposition of endogenous retroviruses. Nature 433 (7024), 430–433.

Feng, Y.Q., Love, R.P., Chelico, L., 2013. HIV-1 viral infectivity factor (Vif) alters processive single-stranded DNA scanning of the retroviral restriction factor APOBEC3G. J. Biol. Chem. 288 (9), 6083–6094.

Goila-Gaur, R., Strebel, K., 2008. HIV-1 Vif, APOBEC, and intrinsic immunity. Retrovirology 5, 51.

Guenzel, C.A., Herate, C., Le Rouzic, E., Maidou-Peindara, P., Sadler, H.A., Rouyez, M.C., Mansky, L.M., Benichou, S., 2012. Recruitment of the nuclear form of uracil DNA glycosylase into virus particles participates in the full infectivity of HIV-1. J. Virol. 86 (5), 2533–2544.

Hoch, J., Lang, S.M., Weeger, M., Stahlhennig, C., Coulibaly, C., Dittmer, U., Hunsmann, G., Fuchs, D., Muller, J., Sopper, S., Fleckenstein, B., Uberla, K.T., 1995. Vpr deletion mutant of simian immunodeficiency virus induces AIDS in rhesus-monkeys. J. Virol. 69 (8), 4807–4813.

Iwabu, Y., Kinomoto, M., Tatsumi, M., Fujita, H., Shimura, M., Tanaka, Y., Ishizaka, Y., Nolan, D., Mallal, S., Sata, T., Tokunaga, K., 2010. Differential anti-APOBEC3G activity of HIV-1 Vif proteins derived from different subtypes. J. Biol. Chem. 285 (46), 35350–35358.

Iwatani, Y., Chan, D.S.B., Liu, L., Yoshii, H., Shibata, J., Yamamoto, N., Levin, J.G., Gronenborn, A.M., Sugiura, W., 2009. HIV-1 Vif-mediated ubiquitination/degradation of APOBEC3G involves four critical lysine residues in its C-terminal domain. Proc. Natl. Acad. Sci. U.S.A. 106 (46), 19539–19544.

Jones, K.L., Roche, M., Gantier, M.P., Begum, N.A., Honjo, T., Caradonna, S., Williams, B.R.G., Mak, J., 2010. X4 and R5 HIV-1 have distinct post-entry requirements for uracil DNA glycosylase during infection of primary cells. J. Biol. Chem. 285 (24), 18603–18614.

Kaiser, S.M., Emerman, M., 2006. Uracil DNA glycosylase is dispensable for human immunodeficiency virus type 1 replication and does not contribute to the antiviral effects of the cytidine deaminase Apobec3G. J. Virol. 80 (2), 875–882.

Kinomoto, M., Kanno, T., Shimura, M., Ishizaka, Y., Kojima, A., Kurata, T., Sata, T., Tokunaga, K., 2007. All APOBEC3 family proteins differentially inhibit LINE-1 retrotransposition. Nucleic Acids Res. 35 (9), 2955–2964.

Klockow, L.C., Sharifi, H.J., Wen, X.Y., Flagg, M., Furuya, A.K.M., Nekorchuk, M., de Noronha, C.M.C., 2013. The HIV-1 protein Vpr targets the endoribonuclease Dicer for proteasomal degradation to boost macrophage infection. Virology 444 (1–2), 191–202.

Kogan, M., Rappaport, J., 2011. HIV-1 accessory protein Vpr: relevance in the pathogenesis of HIV and potential for therapeutic intervention. Retrovirology 8, 25.

Koyama, T., Sun, B.L., Tokunaga, K., Tatsumi, M., Ishizaka, Y., 2013. DNA damage enhances integration of HIV-1 into macrophages by overcoming integrase inhibition. Retrovirology 10, 21.

Kreisberg, J.F., Yonemoto, W., Greene, W.C., 2006. Endogenous factors enhance HIV infection of tissue naive CD4T cells by stimulating high molecular mass APOBEC3G complex formation. J. Exp. Med. 203 (4), 865–870.

Lang, S.M., Weeger, M., Stahlhennig, C., Coulibaly, C., Hunsmann, G., Muller, J., Mullerhermelink, H., Fuchs, D., Wachter, H., Daniel, M.M., Desrosiers, R.C., Fleckenstein, B., 1993. Importance of Vpr for infection of rhesus-monkeys with simian immunodeficiency virus. J. Virol. 67 (2), 902–912.

Langlois, M.A., Neuberger, M.S., 2008. Human APOBEC3G can restrict retroviral infection in avian cells and acts independently of both UNG and SMUG1. J. Virol. 82 (9), 4660–4664.

Le Rouzic, E., Belaidouni, N., Estrabaud, E., Morel, M., Rain, J.C., Transy, C., Margottin-Goguet, F., 2007. HIV1 Vpr arrests the cell cycle by recruiting DCAF1/VprBP, a receptor of the Cul4-DDB1 ubiquitin ligase. Cell Cycle 6 (2), 182–188.

Le Rouzic, E., Benichou, S., 2005. The Vpr protein from HIV-1: distinct roles along the viral life cycle. Retrovirology 2, 11.

Magadan, J.G., Perez-Victoria, F.J., Sougrat, R., Ye, Y.H., Strebel, K., Bonifacino, J.S., 2010. Multilayered mechanism of CD4 downregulation by HIV-1 Vpu involving distinct ER retention and ERAD targeting steps. PLoS Pathog. 6 (4), e1000869.

Mariani, R., Chen, D., Schrofelbauer, B., Navarro, F., Konig, R., Bollman, B., Munk, C., Nymark-McMahon, H., Landau, N.R., 2003. Species-specific exclusion of APOBEC3G from HIV-1 virions by Vif. Cell 114 (1), 21–31.

Marin, M., Rose, K.M., Kozak, S.L., Kabat, D., 2003. HIV-1 Vif protein binds the editing enzyme APOBEC3G and induces its degradation. Nat. Med. 9 (11), 1398–1403.

Mashiach, E., Nussinov, R., Wolfson, H.J., 2010. Fiber Dock: flexible induced-fit backbone refinement in molecular docking. Proteins 78 (6), 1503–1519.

Maudet, C., Sourisce, A., Dragin, L., Lahouassa, H., Rain, J.C., Bouaziz, S., Ramirez, B.C., Margottin-Goguet, F., 2013. HIV-1 Vpr induces the degradation of ZIP and sZIP, adaptors of the NuRD chromatin remodeling complex, by hijacking DCAF1/VprBP. PLoS One 8 (10), e77320.

Muckenfuss, H., Hamdorf, M., Held, U., Perkovic, M., Lower, J., Cichutek, K., Flory, E., Schumann, G.G., Munk, C., 2006. APOBEC3 proteins inhibit human LINE-1 retrotransposition. J. Biol. Chem. 281 (31), 22161–22172.

Nakagawa, T., Mondal, K., Swanson, P.C., 2013. VprBP (DCAF1): a promiscuous substrate recognition subunit that incorporates into both RING-family CRL4 and HECT-family EDD/UBR5 E3 ubiquitin ligases. BMC Mol. Biol. 14, 22.

Newman, E.N.C., Holmes, R.K., Craig, H.M., Klein, K.C., Lingappa, J.R., Malim, M.H., Sheehy, A.M., 2005. Antiviral function of APOBEC3G can be dissociated from cytidine deaminase activity. Curr. Biol. 15 (2), 166–170.

Norman, J.M., Mashiba, M., McNamara, L.A., Onafuwa-Nuga, A., Chiari-Fort, E., Shen, W.W., Collins, K.L., 2011. The antiviral factor APOBEC3G enhances the recognition of HIV-infected primary T cells by natural killer cells. Nat. Immunol. 12 (10), 975–983.

Okumura, A., Alce, T., Lubyova, B., Ezelle, H., Strebel, K., Pitha, P.M., 2008. HIV-1 accessory proteins VPR and Vif modulate antiviral response by targeting IRF-3 for degradation. Virology 373 (1), 85–97.

Priet, S., Gros, N., Navarro, J.M., Boretto, J., Canard, B., Querat, G., Sire, J., 2005. HIV-1-associated uracil DNA glycosylase activity controls dUTP misincorporation in viral DNA and is essential to the HIV-1 life cycle. Mol. Cell 17 (4), 479–490.

Romani, B., Cohen, E.A., 2012. Lentivirus Vpr and Vpx accessory proteins usurp the cullin4-DDB1 (DCAF1) E3 ubiquitin ligase. Curr. Opin. Virol. 2 (6), 755–763.

Rosenstiel, P.E., Chan, J., Snyder, A., Planelles, V., D'Agati, V.D., Klotman, P.E., Klotman, M.E., 2009. HIV-1 Vpr activates the DNA damage response in renal tubule epithelial cells. AIDS 23 (15), 2054–2056.

Schrofelbauer, B., Hakata, Y., Landau, N.R., 2007. HIV-1 Vpr function is mediated by interaction with the damage-specific DNA-binding protein DDB1. Proc. Natl. Acad. Sci. U.S.A. 104 (10), 4130–4135.

Schrofelbauer, B., Yu, Q., Zeitlin, S.G., Landau, N.R., 2005. Human immunodeficiency virus type 1 Vpr induces the degradation of the UNG and SMUG uracil-DNA glycosylases. J. Virol. 79 (17), 10978–10987.

Shatsky, M., Nussinov, R., Wolfson, H.J., 2004. A method for simultaneous alignment of multiple protein structures. Proteins 56 (1), 143–156.

Sheehy, A.M., Gaddis, N.C., Choi, J.D., Malim, M.H., 2002. Isolation of a human gene that inhibits HIV-1 infection and is suppressed by the viral Vif protein. Nature 418 (6898), 646–650.

Tokunaga, K., Greenberg, M.L., Morse, M.A., Cumming, R.I., Lyerly, H.K., Cullen, B.R., 2001. Molecular basis for cell tropism of CXCR4-dependent human immunodeficiency virus type 1 isolates. J. Virol. 75 (15), 6776–6785.

Tristem, M., Marshall, C., Karpas, A., Hill, F., 1992. Evolution of the primate lentiviruses – evidence from Vpx and Vpr. EMBO J. 11 (9), 3405–3412.

Tuncbag, N., Gursoy, A., Nussinov, R., Keskin, O., 2011. Predicting protein–protein interactions on a proteome scale by matching evolutionary and structural similarities at interfaces using PRISM. Nat. Protoc. 6 (9), 1341–1354.

Tuncbag, N., Kar, G., Gursoy, A., Keskin, O., Nussinov, R., 2009. Towards inferring time dimensionality in protein–protein interaction networks by integrating structures: the p53 example. Mol. Biosyst. 5 (12), 1770–1778.

Wang, X., Singh, S., Jung, H.Y., Yang, G.J., Jun, S., Sastry, K.J., Park, J.I., 2013. HIV-1 Vpr protein inhibits telomerase activity via the EDD-DDB1-VPRBP E3 ligase complex. J. Biol. Chem. 288 (22), 15474–15480.

Ward, J., Davis, Z., DeHart, J., Zimmerman, E., Bosque, A., Brunetta, E., Mavilio, D., Planelles, V., Barker, E., 2009. HIV-1 Vpr triggers natural killer cell-mediated lysis